



## Metal-Organic Framework Membranes: From Synthesis to Separation Application

Journal:	<i>Chemical Society Reviews</i>
Manuscript ID:	CS-REV-05-2014-000159.R1
Article Type:	Review Article
Date Submitted by the Author:	10-Jun-2014
Complete List of Authors:	Qiu, Shi Lun; Jilin University, State Key Laboratory of Inorganic Synthesis and Preparative Chemistry, Department of Chemistry Xue, Ming; Jilin University, State Key Laboratory of Inorganic Synthesis and Preparative Chemistry, Department of Chemistry zhu, Guangshan; Jilin University, State Key Laboratory of Inorganic Synthesis and Preparative Chemistry, Department of Chemistry

## REVIEW ARTICLE

# Metal-Organic Framework Membranes: From Synthesis to Separation Application

Cite this: DOI: 10.1039/x0xx00000x

Shilun Qiu,\* Ming Xue and Guangshan Zhu

Received 00th January 2012,  
Accepted 00th January 2012

DOI: 10.1039/x0xx00000x

www.rsc.org/

Metal-organic framework (MOF) materials, which are constructed from metal ions or metal ion clusters and bridging organic linkers, exhibit regular crystalline lattices with relatively well-defined pore structures and interesting properties. As a new class of porous solid materials, MOFs are attractive for a variety of industrial applications including separation membranes – a rapidly developing research area. Many reports have discussed the synthesis and applications of MOFs and MOF thin films, but relatively few have addressed MOF membranes. This critical review provides an overview of the diverse MOF membranes that have been prepared, beginning with a brief introduction to the current techniques for the fabrication of MOF membranes. Gas and liquid separation applications with different MOF membranes are also included. (175 references)

## 1. Introduction

The metal-organic frameworks (MOFs) field has exhibited tremendous growth over the last 15 years. MOFs generally have two main components: the organic linkers and the metal ions. This class of materials has received widespread attention due to the diverse range of linkers and metal ions that can be used, and the fact that the products of their assembly can be crystallised and fully characterised.<sup>1</sup> MOF materials have exceptionally high porosity, uniform but tunable pore sizes and well-defined molecular adsorption site properties. As a new class of porous solid materials, explorations of their performances in separation and purification applications are attracting intense interest from researchers in fields such as chemistry, chemical engineering and materials science.<sup>2-5</sup>

Membrane separation, which has proven very promising in addressing energy and environmental challenges, has experienced rapid growth in the past few decades.<sup>6-8</sup> Compared with traditional gas separation technologies such as PSA/TSA operation, membrane-based gas separation offers great potential application in terms of its lower energy consumption, smaller carbon footprint and easy operation.



*Shilun Qiu received his Ph.D. in chemistry from Jilin University, China, in 1988. He joined the University de Haute-Alsace for postdoctoral research. In 1994, he was promoted to be a full professor in Jilin University. He won the Second Grade Award for the State Natural Science Award of China in 2008. He received the Guest Professorship in Tohoku University, Drexel University, Stockholm University, and is now the Honorary Professor of University of Queensland. His*

*recent research interests focus on the studies of molecular engineering, synthesis, structure and applications of porous materials and membranes, involving zeolites, mesostructured materials, MOFs and COFs.*



*Ming Xue received B.S. (2003) and PhD (2008) degree in Chemistry from Jilin University in China, and joined the University of Texas-Pan American as a visiting scholar during 2007-2008. Currently he works in the Department of Chemistry, State Key Laboratory of Inorganic Synthesis and Preparative Chemistry, Jilin University, as an Associate Professor. His work is focused on multifunctional Metal-Organic*

*Framework materials and Membranes for the applications in adsorption and separation.*

The current market is dominated by polymeric membranes, partially because they have low production costs and exhibit high fluxes and mechanical flexibilities.<sup>9</sup> However, polymer membranes suffer from short lifetimes, low thermal and chemical stabilities and low selectivity. Because of their well-defined, regular pore structure, zeolites materials have been investigated for applications in membrane separations. In addition, the high thermal and chemical stabilities of these materials also make them attractive for separation applications under high temperatures and harsh chemical environments.<sup>10-16</sup> As emerging inorganic and organic hybrid materials, MOF materials are very appealing to be assembled into MOF membranes for gas and liquid separation applications for two reasons: their pores can be rationally controlled by the interplay of both inorganic metal ions and organic linkers, and their pore surfaces can be readily functionalised through a variety of approaches.<sup>17</sup> Generally, the separations are usually based on the size and shape of the molecules to be separated, or on their interaction with the membrane material. For microporous membranes, zeolites and MOFs, there are several factors, such as the limiting pore size and pore size distribution, surface diffusion, capillary condensation, shape selectivity and molecular sieving, contribute to the separations properties. Particularly, preferential adsorption is often the determining factor. In this case, the adsorption of one component in the mixture is stronger and this blocks or hinders the passage of the other components through the membrane pores.<sup>18</sup>

The current MOF research has mainly focused on the discovery and characterisation of new MOF structures. As Fig. 1a shows, the number of publications discussing ‘metal organic frameworks’ has increased significantly during the last decade, with the number of reports on MOF films and membranes experiencing growth in the last five years (Figs. 1b and 1c). Despite being in its infancy, the research progress in this area has already shown that MOF membranes are promising for separation applications.<sup>19</sup> In this review, our discussion focuses on MOF membranes, beginning with a brief introduction to the current methodologies for the fabrication of MOF membranes and such membranes’ performance in gas and liquid separation applications.

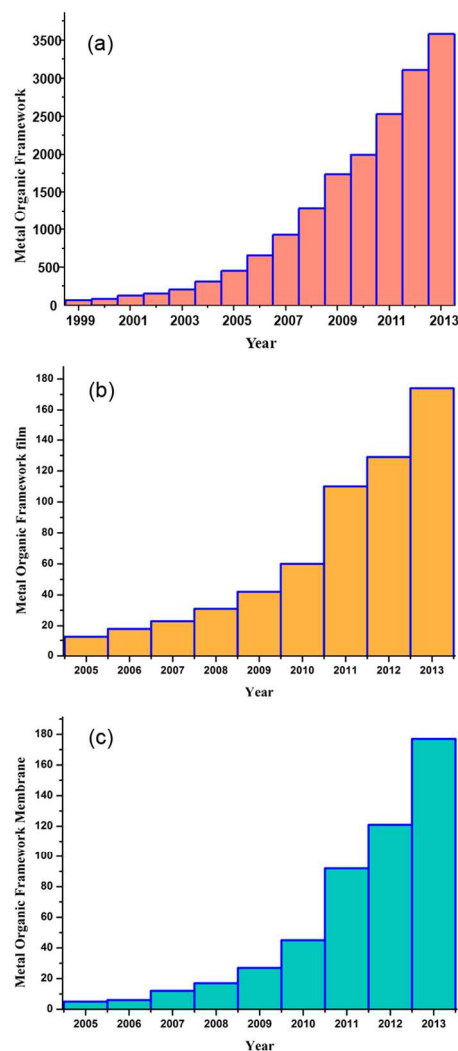


**Fig.1** The number of publications per year: (a) “metal organic framework”, (b) “metal organic frame work film” and (c) “metal organic framework membrane”. Data obtained from Web of science until Dec 25th, 2013.

*Guangshan Zhu studied Chemistry in 1993 and earned his PhD in Chemistry from Jilin University in 1998. He was then appointed as an assistant professor in the Department of Chemistry (Jilin University). In 1999, he worked as a post-doc research associate at Tohoku University in Japan. He has been a full professor since 2001, and holds Cheung Kong Professorship from the Ministry of Education of China and Visiting Professorship in*



*Griffith University (Australia). The current research focuses on the design and synthesis of zeolites, metal-organic frameworks and porous organic frameworks for applications in gas-liquid adsorption, separation, and other advanced applications.*

## 2. Fabrication of MOF Membranes

A wide variety of synthesis methods for obtaining MOF materials have been explored, such as the solvent evaporation diffusion method, the hydro/solvothermal method, the microwave reaction and ultrasonic methods,<sup>20</sup> all of which are less energy intensive than zeolites with high-temperature pressure conditions. The synthesis of MOF membranes can be analogous to that of zeolite membranes, as both are crystalline porous materials. In general, the synthesis of zeolite membranes follows one of two approaches: *in situ* growth or seeded-assisted (secondary) growth.<sup>21</sup>

The fabrication of an MOF film or membrane involves processing a known porous MOF with interesting properties on top of a substrate.<sup>22, 23</sup> In 2005, Fischer *et al.* successfully prepared the first MOF film anchoring a typical MOF-5 building unit to a carboxylic acid-terminated, self-assembled monolayer (SAM) on an Au (111) substrate.<sup>24</sup> In 2007, Caro *et al.* reported the *in situ* crystallisation of Mn(HCO<sub>2</sub>)<sub>2</sub> crystals on

different porous supports and found that the property of the surface significantly influenced crystal density.<sup>25</sup> Bein *et al.* reported an oriented growth of MOFs (HKUST-1, MIL-53 and MIL-88) on SAM-modified metal substrates.<sup>26, 27</sup> Gascon *et al.* achieved the synthesis of much denser HKUST-1 membranes on porous alumina supports through a seeded growth technique. However, no gas permeation results have been reported.<sup>28-30</sup> All of these pioneering efforts indicate that the requirements for MOF films and membranes are notably different. It is more challenging to fabricate a continuous and defect-free MOF membrane. For instance, MOF membranes require that crystals are well-intergrown to minimise nonselectivity. The presence of pinhole defects, grain boundary defects, intracrystalline and intercrystalline cracks, can significantly mar the separation performance of the membrane formation.<sup>31, 32</sup> Additional requirements that become critical when considering the commercial application of MOF membranes include the stability of MOF materials in harsh environments and the repeatability of performance over a long period of operation. In contrast, MOF films do not need to fulfil these requirements for use in sensor applications. In 2009, the first MOF membrane for gas separation – based on MOF-5 supported on a porous alumina substrate – was published by Lai and Jeong *et al.*<sup>33</sup> We prepared a HKUST-1 MOF membrane on a copper net *in situ*, showing a high permeability and selectivity for hydrogen. Tsapatsis *et al.* reported a Cu<sub>2</sub>(bpe) MOF membrane prepared using a secondary growth method.<sup>34</sup> Caro *et al.* synthesised a typical ZIF-8 membrane using a microwave-assisted solvothermal method.<sup>35</sup> These reports demonstrate the feasibility of fabricating MOF membranes for use in separation applications. Thus far, various functionalised and nonfunctionalised substrates such as silica, alumina, titania, graphite, metal nets, porous ZnO supports, or nylon have been used as foundations for the deposition of MOF films and the preparation of MOF membranes. Many creative methods have been used in the fabrication of MOF films and membranes such as direct growth, layer-by-layer growth, secondary growth, chemical solution deposition, electrospinning technology and microwave.<sup>36</sup>

In the following section, only methods for synthesising MOF membranes are discussed. For MOF film fabrication methods, interested readers may note recent review articles.<sup>37-42</sup>

## 2.1 Direct growth on Unmodified Supports

Direct growth is defined as when the substrate is immersed in the growth solution without any crystals previously attached to the surface. The nucleation, growth and intergrowth of crystals on the substrate all happen during the same fabrication step.

Lai and Jeong *et al.* chose MOF-5 and prepared it as a layer on top of a porous alumina without substrate modification through *in situ* solvothermal synthesis. This is the first example of a continuous and well-intergrown MOF membrane (Fig. 2).<sup>33</sup> The mother solution was sealed and heated to 105°C and membranes of different thicknesses were obtained at different synthesis times. For an MOF based on ligands with carboxylic acid groups, covalent bonds are very likely to form between the carboxyl groups of ligands and the hydroxyl groups at the alumina support's surface.<sup>43</sup>

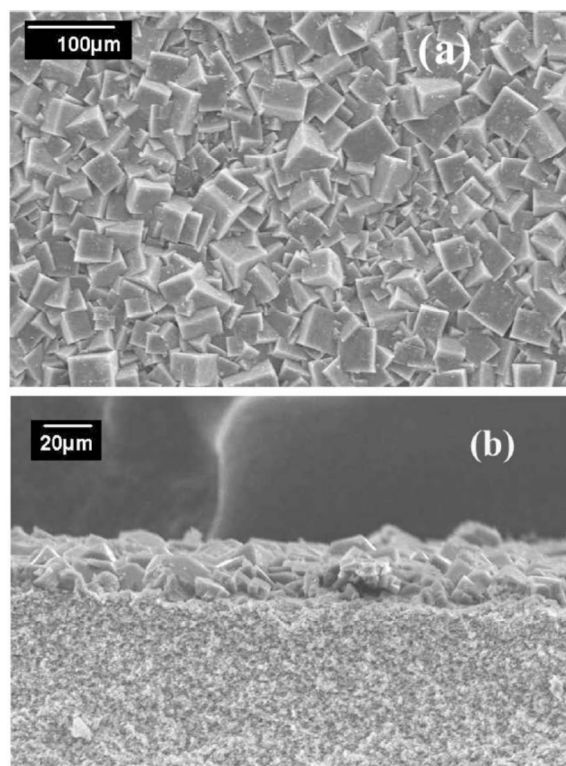


**Fig. 2** SEM images of MOF-5 membrane: (a) top view, (b) cross section (Adapted with permission from ref.<sup>33</sup>).

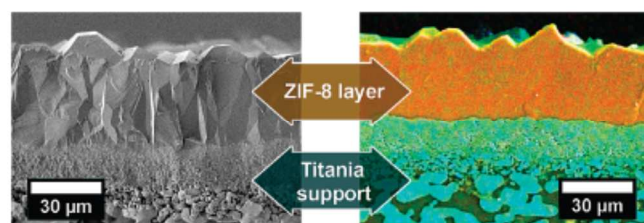


**Fig. 3** (left) SEM image of the cross section of a simply broken ZIF-8 membrane; (right) EDXS mapping of the sawn and polished ZIF-8 membrane – orange is Zn and cyan is Ti (Adapted with permission from ref.<sup>35</sup>).

ZIF-8 is also a typical zeolitic MOF crystalline porous material with a sodalite (SOD) topology. The 3.4 Å small aperture (which is within the range of a few gas molecules in kinetic diameter), the remarkable thermal and chemical stability and the simple synthetic steps make it an ideal candidate. Caro *et al.* synthesised ZIF-8 nanocrystals at room temperature, replacing the solvents of dimethylformamide (DMF) and aqueous methanol with pure methanol. By applying this improved synthetic protocol in membrane preparation, they directly synthesised a crack-free, dense, polycrystalline layer of ZIF-8 on a porous titania support using a microwave-assisted solvothermal method (Fig. 3).<sup>35</sup> For other ZIFs, such as ZIF-69, Lai *et al.* fabricated them on alumina without substrate modification using the *in situ* solvothermal method.<sup>44</sup> However, it remains difficult to prepare continuous MOF membranes by a direct solvothermal synthesis route because the heterogeneous nucleation of MOF crystals on support surfaces is not efficient. As we know, the MOF synthesis involves coordination bonding between metal centres and organic

ligands. Therefore, a particularly favourable case is encountered when the substrate is made of the same metal as the MOF to be grown. This scenario can enhance the interfacial bonding between MOFs and substrates. In 2009, our group reported an HKUST-1 membrane grown on a copper net substrate by means of a ‘twin copper source’ technique. The copper net (400 mesh) was first oxidised at 100°C until the colour changed from yellow to green, indicating the presence of copper oxide. Subsequently, the modified copper net was placed in an auto-clave filled with an HKUST-1 mother solution and stored at 120°C for 3 days. As Fig. 4 shows, a defect-free, homogeneous membrane with a thickness of approximately 60  $\mu\text{m}$  was obtained.<sup>45</sup>

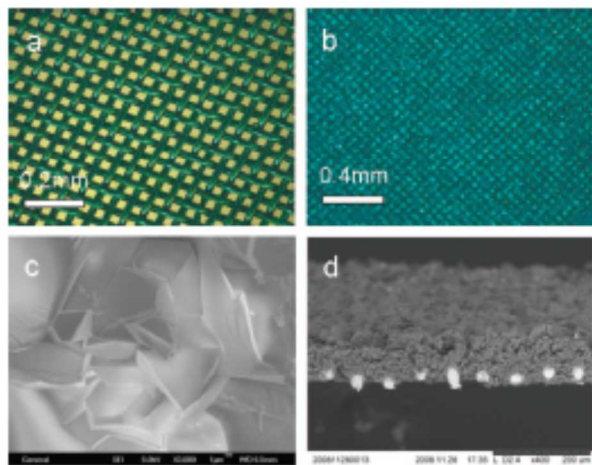


**Fig. 4** Optic micrographs of the (a) copper net and (b) net-supported Cu<sub>3</sub>(BTC)<sub>2</sub> membrane. SEM image of (c) the surface and (d) a cross-section of the membrane (Adapted with permission from ref.<sup>45</sup>).

Furthermore, a simple method of ‘single metal source’ has been developed to facilitate the preparation of a homochiral MOF membrane on a nickel net. The nickel net played a dual role in the synthesis process as the only nickel source added to the reaction system and as a substrate supporting the membrane. The nickel net substrate was placed horizontally in a Teflon-lined autoclave, and it reacted with the organic ligands in a solution of a suitable concentration. The Ni<sub>2</sub>(L-asp)<sub>2</sub>(bipy) crystals first grew around the wires of the nickel net and then continued to intergrow as time passed (Fig. 5). Because the nickel net was the only metal source in the reaction system, the growth process stopped once a layer of the crystal film had formed, making the final membrane thinner and continuous.<sup>46</sup>

## 2.2 Direct Growth on Modified Supports

Poor membrane substrate bonding is a common challenge facing MOF membranes, and few were reported without modifying the porous support. One effective strategy is to chemically modify the supports to improve heterogeneous nucleation and the direct growth of the MOF membranes. A SAM serves as a general method that plays a dominant role in designing chemical and physical functionalities at surfaces on a molecular level.<sup>47-49</sup> A broad range of inorganic compounds including calcium carbonate, lead sulphide, zinc, titanium iron oxides, and zeolites have been grown as thin films using the SAM method.<sup>50-56</sup>

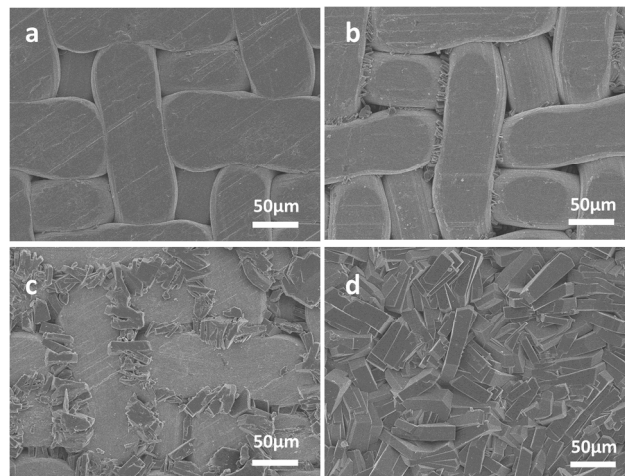


**Fig. 5** Top view SEM pictures of Ni<sub>2</sub>(L-asp)<sub>2</sub>(bipy) membranes grown for a) 1 h, b) 2 h, c) 3 h, d) 4 h at 150°C (Adapted with permission from ref.<sup>46</sup>).

Caro *et al.* reported a covalent functionalization strategy for preparing a molecular sieve ZIF-90 membrane using 3-aminopropyltriethoxysilane (APTES) as covalent linkers between the ZIF-90 layer and Al<sub>2</sub>O<sub>3</sub> support (Fig. 6). In the first step, the ethoxy groups of the APTES reacted with the hydroxyl groups at the Al<sub>2</sub>O<sub>3</sub> support's surface. In the second step, the amino groups reacted with the aldehyde groups of ICA via an imines condensation. Subsequently, the nucleation and crystal growth for the ZIF-90 begin at these fixed sites on the surfaces of the porous ceramic supports. After solvothermal reaction for 18 h at 100°C, the surface of the APTES-modified support was completely covered with well-intergrown rhombic dodecahedrons and a compact ZIF-90 layer with a thickness of about 20  $\mu\text{m}$ . The presence of the free aldehyde groups in the framework allowed the covalent functionalization of ZIF-90 with the amine groups via an imine condensation reaction.<sup>57</sup> They also reported ZIF-22 membranes on alumina supports modified with APTES as a covalent linker between the ZIF crystals and the alumina supports, promoting heterogeneous nucleation and growth.<sup>58</sup>

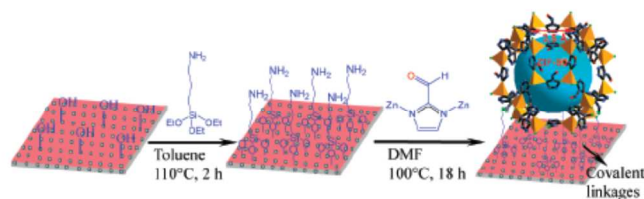


**Fig. 6** Scheme for preparing ZIF-90 membranes using 3-aminopropyltriethoxysilane (APTES) as a covalent linker between a ZIF-90 membrane and an Al<sub>2</sub>O<sub>3</sub> support via an imine condensation reaction (Adapted with permission from ref.<sup>57</sup>).

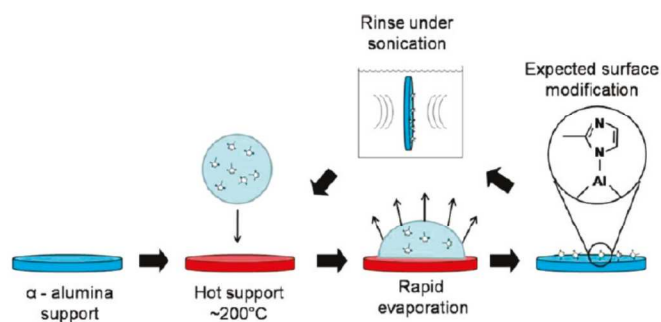


**Fig. 7** Illustration of the substrate modification process (Adapted with permission from ref.<sup>59</sup>).

Jeong *et al.* also reported a potentially general method for ZIF membrane fabrication using a simple support modification technique. In 2010, ZIF-8 and ZIF-7 membranes were prepared, based on the covalent linkage of imidazole ligands to supports via an Al-N bond. As Fig. 7 shows, the supports were thermally modified through the rapid evaporation of a solution (the organic linker: 2-methylimidazole in methanol for ZIF-8 or benzimidazole in methanol for ZIF-7) on the surface of hot alumina ( $\sim 200^\circ\text{C}$ ). The solvent evaporated quickly, leaving organic linkers covalently attached to the alumina surface. The solvothermal growth of supports modified in this way was found to yield continuous and well-intergrown ZIF membranes *in situ*.<sup>59</sup>

In 2012, a convenient method for preparing MOF membranes has been reported. First, a poly(methyl methacrylate) (PMMA) membrane was spin-coated on a template substrate, which could be any solid surface of metal, plastic, etc. Then, the PMMA surface was hydrolysed by concentrated sulphuric acid and converted into PMAA. Finally, the PMMA-PMAA coated substrate was immersed in an MOF precursor solution in autoclaves for a suitable reaction time. For the further preparation of a free-standing MOF membrane, the as-synthesised MOF membrane can be separated from the substrate by dissolving the PMMA-PMAA in chloroform (Fig. 8). Using this method, intact free-standing MOF membranes of various sizes, shapes and thicknesses – from hundreds of nanometres to hundreds of micrometres – have been synthesised. This MOF membrane fabrication method is simple, convenient and can be readily applied to a variety of other material compositions to synthesise functional membranes with diverse micropore structures, thus opening up a host of opportunities for developing new functional nano devices.<sup>60</sup>

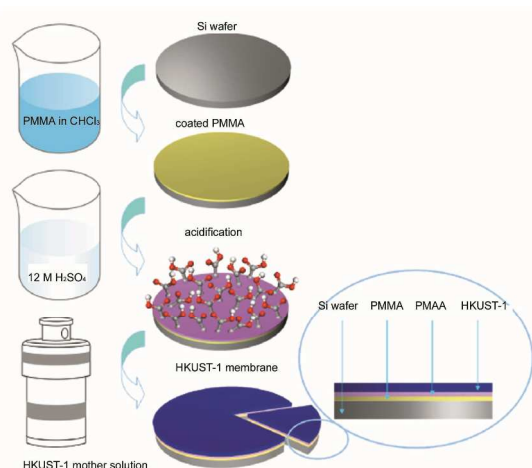


**Fig. 8** Schematic illustration of the preparation procedure for free-standing HKUST-1 membrane (Adapted with permission from ref.<sup>60</sup>).

As mentioned, the process of preparing MOF membranes is not straightforward and often requires multiple steps because the heterogeneous nucleation and growth of MOF crystals on porous supports are not generally favoured.

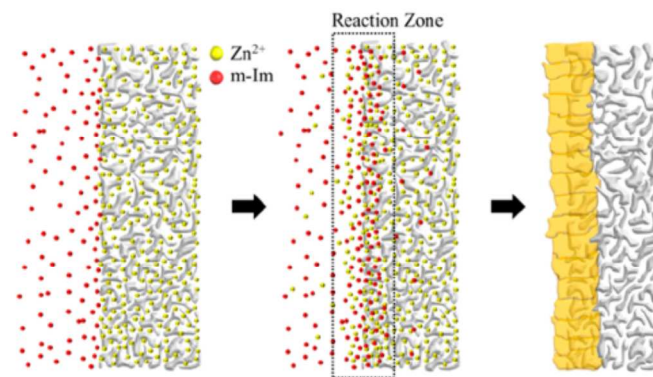


**Fig. 9** Schematic illustration of membrane synthesis using the counter-diffusion-based *in situ* method (Adapted with permission from ref.<sup>61</sup>).

More recently, Jeong *et al.* reported a simple one-step *in situ* method based on a counter-diffusion concept to prepare well-intergrown ZIF-8 membranes. As Fig. 9 shows, porous  $\alpha\text{-Al}_2\text{O}_3$  supports were soaked in a metal ion solution and then subjected to solvothermal growth in a ligand solution. On contact, the concentration gradients enabled metal ions and ligand molecules to diffuse from the support into the solution and from the solution into the support, respectively. Relatively high concentrations of both metal ions and ligand molecules were maintained in the vicinity of the support ('reaction zone') during the solvothermal treatment. After 30 min, the crystal growth appeared to be complete, with the grain size and the film thickness of ca.  $1.5\ \mu\text{m}$  not changing, even with further growth – a difficulty of preparation by *in situ* method.<sup>61</sup>

### 2.3 Secondary Growth

The direct growth method has support material type limitations, and thus is usually applied after the support surface has been modified through a series of complex operations. It is relatively easy to control the final orientation and obtain a dense and continuous membrane free from cracks or intercrystalline gaps using the seed-assisted growth method, in which the seeding procedure is of vital importance. Several seeding techniques are widely used these days including rubbing, dip coating, wiping, spin coating and heating. Tsapatsis *et al.* reported the synthesis of a microporous MOF membrane through manually rubbing the seed crystals onto PEI-coated alumina, but *in situ* growth did not yield membrane-quality films. Their results showed *b*-out-of-plane orientation in their membrane and demonstrated the use of the crystallographic preferential orientation (CPO) indexing method and pole figure analysis. Although the seeds used for secondary growth were randomly oriented, the investigators attributed the membrane orientation to faster crystal growth in the *b* direction (Fig. 10).<sup>34</sup>

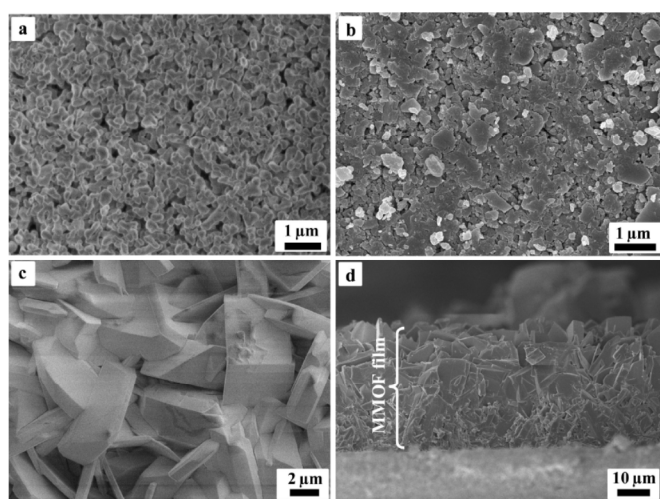


**Fig. 10** SEM images at different stages of MOF membrane growth: (a)  $\alpha$ -alumina support, (b) seed layer, (c) membrane (top view) and (d) membrane (cross-section view) (Adapted with permission from ref.<sup>34</sup>).

Nanosized MOF seed crystals are also important in preparing MOF membranes through the seed-assisted growth method. We reduced the size of the Ln-MOF crystals to diameters of around 100 nm by adding capping reagents with the same chemical functionality as the linkers. Sodium carboxylates (sodium formate, sodium acetate or sodium oxalate) were used as the capping reagent to control the resulting MOF crystal size and morphology (Fig. 11).<sup>62</sup>

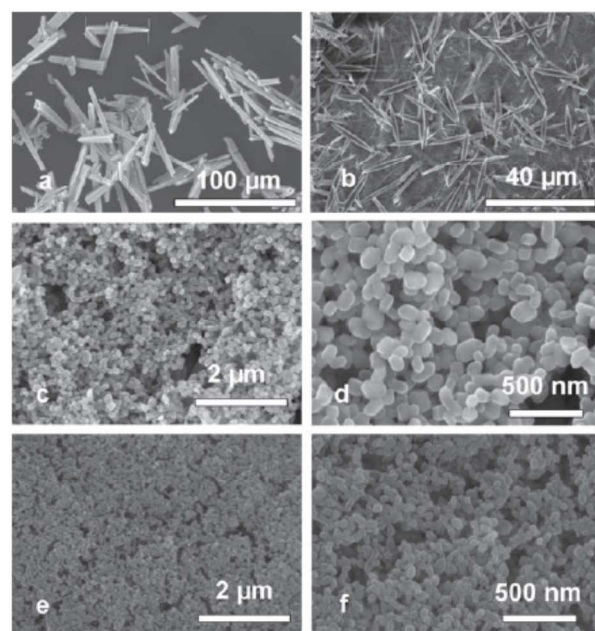


**Fig. 11** SEM images of Ln-MOFs crystals synthesised: (a) without capping reagent; with the addition of (b) sodium oxalate, (c,d) sodium formate and (e,f) sodium acetate (Adapted with permission from ref.<sup>62</sup>).

In 2012, we prepared a continuous  $\text{NH}_2$ -MIL-53(AI) membrane assisted by colloidal seeds on macroporous glass frit discs. First, an as-prepared colloidal seed suspension was dropwise deposited on the pretreated macroporous glass frit support and then dried in air at room temperature overnight to form a seed layer. The seeded supports were placed vertically in Teflon-lined autoclaves containing a mother solution and then subjected to a further solvothermal treatment at 423 K for three days to obtain a well-intergrown MOF membrane.<sup>63</sup>

Finding a versatile method suitable for different kinds of supports that can meet the requirements of forming a uniform seed layer with controllable thickness on the support surface has remained a great challenge. To meet the demand, we adopted a novel method using the electrospinning technique as a means of seeding. This approach can be applied to various types of supports, especially tubes. With respect to other conventional seeding methods, this low-cost technique has a wider range of applications with the possibility of large-area processing.

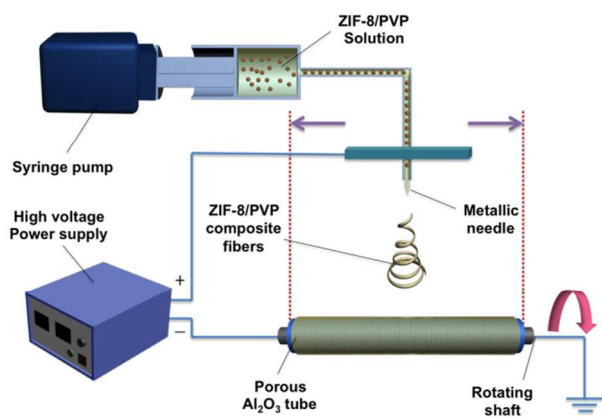


**Fig. 12** Schematic diagram of the electrospinning process for seeding a support (porous  $\text{Al}_2\text{O}_3$  tube) (Adapted with permission from ref. <sup>64</sup>).

A general schematic representation of the electrospinning process is shown in Fig. 12. The electrospinning solution prepared with ZIF-8 nanoparticles, PVP and methanol are first loaded into the syringe, which is connected to a hose with a capillary tip. The electrospinning rate is controlled by a pump. A high voltage is then applied to the metallic tip to draw the viscous solution into the fibres. The macroporous  $\text{SiO}_2$  support then serves as the collector, together with aluminium foil, receiving non-woven mats of composite fibres. The tubular supports are fixed on a rotating shaft and the spinner moves periodically with constant speed. Thus, the electrospun fibres are uniformly wrapped around the support's outer surface.<sup>64</sup> To certify the effectiveness of this method, we have developed it to synthesise different types of microporous membranes and films on various substrates: a zeolite NaA and a pure-silica-zeolite Beta membrane were synthesised on  $\text{Al}_2\text{O}_3$  tubes; a zeolite NaY membrane was synthesised on a stainless steel net; and a MOF JUC-32 film was synthesised on a silica disc – all of which indicate the potential of this method for practical applications.<sup>65</sup>

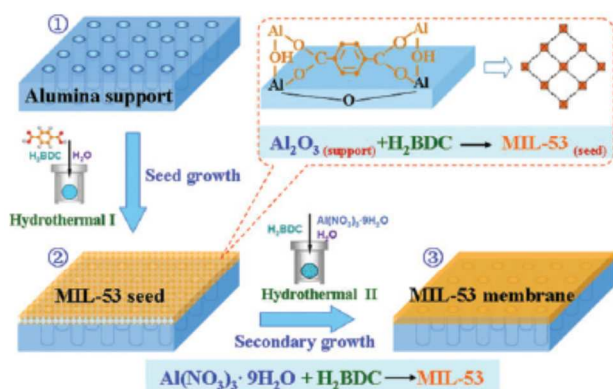


**Fig. 13** Schematic diagram of preparing the MIL-53 membrane on an alumina support *via* the reactive seeding method (Adapted with permission from ref. <sup>66</sup>).

Like directly synthesis method, the seeding step can be carried during *in situ* growth as well. This facile technique is called reactive seeding (RS).<sup>66</sup> In this method, the seed layer was produced by the

reaction between the inorganic support and the organic precursor in a single stage (Fig. 13). The RS method proved to be of critical importance to achieve a uniform, thin and well inter-grown MOF membrane.

The layer-by-layer (LBL) growth method has been developed and demonstrated for thin films of HKUST-1, the mixed-ligands, and pillared-layered MOFs. In 2007, Wöll *et al.* demonstrated the first successful crystalline HKUST-1 thin film by applying LBL.<sup>67</sup> In 2010, the Langmuir-Blodgett (LB) approach has been adopted for MOF monolayer growth by Kitagawa *et al.*<sup>68</sup> It relies on MOF layers made in a LB apparatus that are transferred one after another onto a silicon substrate with intermediate rinsing steps. The layers stack by weak interactions, such as  $\pi$  stacking between pendant groups in a manner similar to interdigitated MOFs. NAFS-1 was made of cobalt-containing porphyrine units (CoTCCP) linked together by binuclear copper paddle-wheel units to form a 2D array. Pyridine molecules bind the axial position of the copper ions perpendicularly to the 2D layers and ensure correct  $\pi$  stacking. The individual sheets are remarkably ordered, with an average tilt angle of  $0.3^\circ$  parallel to the substrate, and the overall thickness of the film corresponds to deposition of one single layer at each cycle.

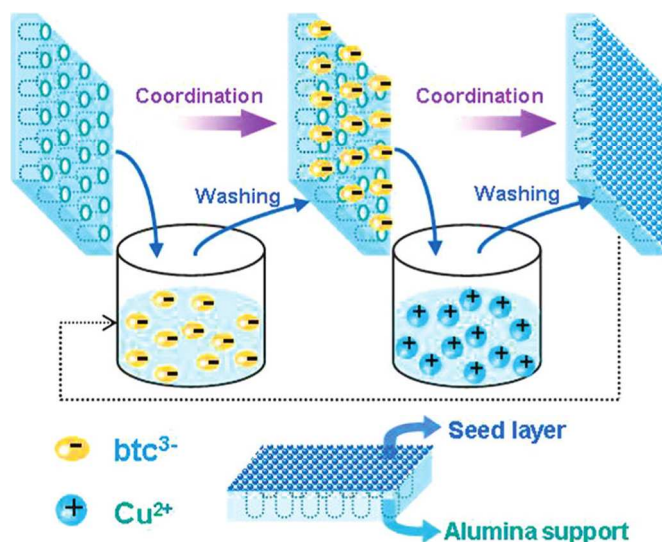


**Fig. 14** Schematic diagram of step-by-step deposition of  $\text{btc}^{3-}$  and  $\text{Cu}^{2+}$  on alumina support. (Adapted with permission from ref. <sup>69</sup>)

As discussed above, LBL method is always used to synthesize MOF films but not membranes because this method can't produce a defect-free membrane layer. For the preparation of MOF membranes, the LBL can be used for a seeding step. In 2010, the LBL seeding technique was applied for the first time to fabricate a uniform seed layer on a porous alumina support by Jin *et al.* As shown in Fig. 14, the integrated HKUST-1 membrane was synthesized on the seeded support by secondary growth.<sup>69</sup>

## 2.4 Post-Synthesis Modification

To the reinforcement of MOF structures, some post-synthesis processes should improve the stability of MOF material recently. This method can also be used to adjust the pore structures and interaction between the channel and separation molecules by modifying the cages' inner walls. The representative work was done

by Caro *et al.*,<sup>70</sup> who conducted the covalent post-functionalization of a ZIF-90 molecular sieve membrane by imine condensation with ethanolamine. The obtained membrane exhibited a significant increase in the H<sub>2</sub> recycling, which is discussed subsequently. Recently, Yang *et al.* reported that the hydrothermal stability of ZIF-8 can be remarkably improved via the shell-ligand-exchange-reaction (SLER),<sup>71</sup> which takes advantage of the hydrophobicity (water-repellent) and steric hindrance effects of 5,6-dimethylbenzimidazole (DMBIM) (Fig. 15). After SLER treatment, the ZIF-8-DMBIM retains the structural characteristics of ZIF-8 with improved application performance in adsorption and membrane separation. In addition to ZIF-8, the SLER methodology was also successfully applied to stabilise other types of ZIFs, e.g. ZIF-7 and ZIF-93. The stabilised ZIF materials are expected to be suitable for various applications under aqueous conditions such as adsorbents, membranes and heterogeneous catalysts.

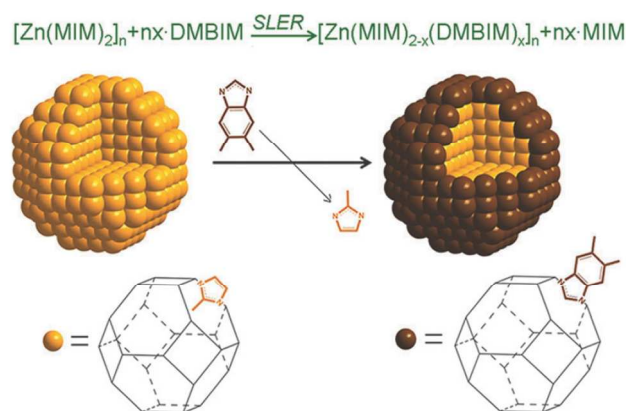


Fig. 15 Schematic representation of the shell-ligand-exchange-reaction (SLER) process for ZIF-8 (Adapted with permission from ref. <sup>71</sup>).

**Table 1.** Summary of MOF membranes for H<sub>2</sub> separation

MOF	Pore size (Å)	Substrate	Application	Temp. (°C)	Separation factor	H <sub>2</sub> permeance (molm <sup>-2</sup> s <sup>-1</sup> Pa <sup>-1</sup> )	Ref.
Cu <sub>2</sub> (bza) <sub>4</sub> (pyz)	2	Al <sub>2</sub> O <sub>3</sub> sheet	H <sub>2</sub>	RT	H <sub>2</sub> /N <sub>2</sub> (10*) H <sub>2</sub> /CH <sub>4</sub> (19*)	6.88×10 <sup>-9</sup>	72
ZIF-7	3	α-Al <sub>2</sub> O <sub>3</sub> disks	H <sub>2</sub>	20-200	H <sub>2</sub> /N <sub>2</sub> (7.7) H <sub>2</sub> /CH <sub>4</sub> (5.9)	8.00×10 <sup>-8</sup>	73
ZIF-7	3	α-Al <sub>2</sub> O <sub>3</sub> disks	H <sub>2</sub>	220	H <sub>2</sub> /CO <sub>2</sub> (13.6) H <sub>2</sub> /N <sub>2</sub> (18) H <sub>2</sub> /CH <sub>4</sub> (14)	4.55×10 <sup>-8</sup>	74
ZIF-7	3	α-Al <sub>2</sub> O <sub>3</sub> disks	H <sub>2</sub>	200	H <sub>2</sub> /CO <sub>2</sub> (8.4)	9.00×10 <sup>-9</sup>	75
ZIF-22	3	TiO <sub>2</sub> disks	H <sub>2</sub>	50	H <sub>2</sub> /CO <sub>2</sub> (7.2) H <sub>2</sub> /N <sub>2</sub> (6.4) H <sub>2</sub> /O <sub>2</sub> (6.4) H <sub>2</sub> /CH <sub>4</sub> (5.2)	1.60×10 <sup>-7</sup>	58
ZIF-8	3.4	TiO <sub>2</sub> disks	H <sub>2</sub>	RT	H <sub>2</sub> /CH <sub>4</sub> (11.2)	6.70×10 <sup>-8</sup>	35
ZIF-8	3.4	nylon support	H <sub>2</sub>	RT	H <sub>2</sub> /N <sub>2</sub> (4.3)	1.97×10 <sup>-6</sup>	76
ZIF-8	3.4	porous SiO <sub>2</sub>	H <sub>2</sub>	RT	H <sub>2</sub> /CO <sub>2</sub> (7.3) H <sub>2</sub> /N <sub>2</sub> (4.9) H <sub>2</sub> /CH <sub>4</sub> (4.8)	3.00×10 <sup>-7</sup>	64
ZIF-8	3.4	Hollow fibre	H <sub>2</sub>	RT	H <sub>2</sub> /N <sub>2</sub> (10.3) H <sub>2</sub> /CH <sub>4</sub> (10.4)	2.00×10 <sup>-7</sup>	59
ZIF-8	3.4	α-Al <sub>2</sub> O <sub>3</sub> disks	H <sub>2</sub>	RT	H <sub>2</sub> /N <sub>2</sub> (11.6) H <sub>2</sub> /CH <sub>4</sub> (13)	1.70×10 <sup>-7</sup>	77
Zn <sub>2</sub> (cam) <sub>2</sub> dabco	3×3.5	porous ZnO	H <sub>2</sub>	RT	H <sub>2</sub> /N <sub>2</sub> (19.1) H <sub>2</sub> /CH <sub>4</sub> (14.7)	2.70×10 <sup>-8</sup>	78
ZIF-90	3.5	α-Al <sub>2</sub> O <sub>3</sub> disks	H <sub>2</sub>	25-225	H <sub>2</sub> /CO <sub>2</sub> (11.7) H <sub>2</sub> /N <sub>2</sub> (7.3) H <sub>2</sub> /CH <sub>4</sub> (15.3) H <sub>2</sub> /C <sub>2</sub> H <sub>4</sub> (62.8)	2.50×10 <sup>-7</sup>	57
ZIF-90(post)	3.5	α-Al <sub>2</sub> O <sub>3</sub> disks	H <sub>2</sub>	25-225	H <sub>2</sub> /CO <sub>2</sub> (15.3) H <sub>2</sub> /N <sub>2</sub> (15.8) H <sub>2</sub> /CH <sub>4</sub> (18.9)	1.90~2.10×10 <sup>-7</sup>	70
Cuhfipbb	3.5	α-Al <sub>2</sub> O <sub>3</sub> disk	H <sub>2</sub>	25-200	H <sub>2</sub> /N <sub>2</sub> (22*) H <sub>2</sub> /CO <sub>2</sub> (4*) CO <sub>2</sub> /N <sub>2</sub> (5*)	1.50×10 <sup>-8</sup>	34
ZIF-95	3.7	α-Al <sub>2</sub> O <sub>3</sub> disks	H <sub>2</sub>	RT	H <sub>2</sub> /CO <sub>2</sub> (25.7) H <sub>2</sub> /CO <sub>2</sub> (9.5)	1.95×10 <sup>-6</sup>	79
ZIF-78	3.8	porous ZnO	H <sub>2</sub>	RT	H <sub>2</sub> /N <sub>2</sub> (5.7) H <sub>2</sub> /CH <sub>4</sub> (6.4)	1.00×10 <sup>-7</sup>	80
CAU-1	3.8	α-Al <sub>2</sub> O <sub>3</sub> tube	H <sub>2</sub>	RT	H <sub>2</sub> /CO <sub>2</sub> (12.3) H <sub>2</sub> /N <sub>2</sub> (10.33) H <sub>2</sub> /CH <sub>4</sub> (10.4)	1.00×10 <sup>-7</sup>	81

Journal Name								ARTICLE
Zn <sub>2</sub> (bdc) <sub>2</sub> dabco	7.5	$\alpha$ -Al <sub>2</sub> O <sub>3</sub> disk	H <sub>2</sub>	RT	H <sub>2</sub> /CO <sub>2</sub> (12.1)	2.70×10 <sup>-6</sup>	82	
NH <sub>2</sub> -MIL-53(Al)	7.5Å	porous SiO <sub>2</sub>	H <sub>2</sub>	15-80	H <sub>2</sub> /CO <sub>2</sub> (30.9) H <sub>2</sub> /N <sub>2</sub> (23.9) H <sub>2</sub> /CH <sub>4</sub> (20.7) H <sub>2</sub> /CO <sub>2</sub> (*4)	2.00×10 <sup>-6</sup>	63	
MIL-53(Al)	7.3×7.7	$\alpha$ -Al <sub>2</sub> O <sub>3</sub> disks	H <sub>2</sub>	RT	H <sub>2</sub> /N <sub>2</sub> (*2.5) H <sub>2</sub> /CH <sub>4</sub> (*2.2)	5.00×10 <sup>-7</sup>	66	
MOF-5	7.8	$\alpha$ -Al <sub>2</sub> O <sub>3</sub> discs	H <sub>2</sub>	RT	H <sub>2</sub> , CH <sub>4</sub> , N <sub>2</sub> , CO <sub>2</sub> , SF <sub>6</sub> Follow Knudsen diffusion	3.00×10 <sup>-6</sup>	33	
MOF-5	7.8	$\alpha$ -Al <sub>2</sub> O <sub>3</sub> discs	H <sub>2</sub>	RT	H <sub>2</sub> /CO <sub>2</sub> (2.5) H <sub>2</sub> /N <sub>2</sub> (2.7) H <sub>2</sub> /CH <sub>4</sub> (2)	8.00×10 <sup>-7</sup>	83	
MOF-5	7.8	$\alpha$ -Al <sub>2</sub> O <sub>3</sub> disks	H <sub>2</sub>	RT	H <sub>2</sub> /N <sub>2</sub> (4*) H <sub>2</sub> /CO <sub>2</sub> (4.1*)	4.30×10 <sup>-7</sup>	84	
HKUST-1	9	copper net	H <sub>2</sub>	RT	H <sub>2</sub> /N <sub>2</sub> (7) H <sub>2</sub> /CO <sub>2</sub> (6.8) H <sub>2</sub> /CH <sub>4</sub> (5.9)	1.50×10 <sup>-6</sup>	45	
HKUST-1	9	PSF	H <sub>2</sub>	RT/60	H <sub>2</sub> /CO <sub>2</sub> (7.2) H <sub>2</sub> /C <sub>3</sub> H <sub>8</sub> (5.7)	7.90×10 <sup>-8</sup>	85	
HKUST-1	9	$\alpha$ -Al <sub>2</sub> O <sub>3</sub> disks	H <sub>2</sub>	RT	H <sub>2</sub> /CO <sub>2</sub> (4.6) H <sub>2</sub> /N <sub>2</sub> (3.7) H <sub>2</sub> /CH <sub>4</sub> (3)	4.00~6.00×10 <sup>-7</sup>	69	
HKUST-1	9	porous SiO <sub>2</sub> metal nets	H <sub>2</sub>	25-60	H <sub>2</sub> /CO <sub>2</sub> (9.24) H <sub>2</sub> /N <sub>2</sub> (8.91) H <sub>2</sub> /CH <sub>4</sub> (11.2)	1.00×10 <sup>-6</sup>	60	
HKUST-1	9	$\alpha$ -Al <sub>2</sub> O <sub>3</sub> tube	H <sub>2</sub>	RT	H <sub>2</sub> /CO <sub>2</sub> (13.6) H <sub>2</sub> /N <sub>2</sub> (8.66) H <sub>2</sub> /CH <sub>4</sub> (6.19)	4.00×10 <sup>-8</sup>	86	
Cu(bipy) <sub>2</sub> (SiF <sub>6</sub> )	9.5	porous SiO <sub>2</sub>	H <sub>2</sub>	RT	H <sub>2</sub> /CO <sub>2</sub> (8.0) H <sub>2</sub> /N <sub>2</sub> (6.8) H <sub>2</sub> /CH <sub>4</sub> (7.5)	2.70×10 <sup>-7</sup>	87	
MOF-74	11	$\alpha$ -Al <sub>2</sub> O <sub>3</sub> disks	H <sub>2</sub>	RT	H <sub>2</sub> /CO <sub>2</sub> (9.1) H <sub>2</sub> /N <sub>2</sub> (3.1) H <sub>2</sub> /CH <sub>4</sub> (2.9)	1.00×10 <sup>-5</sup>	88	

\* Idea separation factor

**Table 2.** Summary of MOF membranes for CO<sub>2</sub> separation

MOF	Pore size (Å)	Substrate	Application	Temp. (°C)	Separation factor	Permeance (molm <sup>-2</sup> s <sup>-1</sup> Pa <sup>-1</sup> )	Ref.
Cu <sub>2</sub> (bza) <sub>4</sub> (pyz)	2	Al <sub>2</sub> O <sub>3</sub> sheet	CO <sub>2</sub>	RT	CO <sub>2</sub> /CO (10*) CO <sub>2</sub> /CH <sub>4</sub> (19*)	9.38×10 <sup>-5<math>\delta</math></sup>	72
bio-MOF-14	1.6-4	$\alpha$ -Al <sub>2</sub> O <sub>3</sub> tube	CO <sub>2</sub>	RT	CO <sub>2</sub> /CH <sub>4</sub> (3.5)	4.10×10 <sup>-6</sup>	89
bio-MOF-13	3.2-6.4	$\alpha$ -Al <sub>2</sub> O <sub>3</sub> tube	CO <sub>2</sub>	RT	CO <sub>2</sub> /CH <sub>4</sub> (3.8)	3.10×10 <sup>-6</sup>	89
ZIF-8	3.4	$\alpha$ -Al <sub>2</sub> O <sub>3</sub> tube	CO <sub>2</sub>	RT	CO <sub>2</sub> /CH <sub>4</sub> (7)	1.90×10 <sup>-5</sup>	90
[Cu <sub>2</sub> L <sub>2</sub> P] <sub>n</sub>	3.5	TiO <sub>2</sub> and $\alpha$ -Al <sub>2</sub> O <sub>3</sub> discs	CO <sub>2</sub>	RT	CO <sub>2</sub> /CH <sub>4</sub> (4-5)	1.50×10 <sup>-8</sup>	91
Co <sub>3</sub> (HCOO) <sub>6</sub>	5.5	Porous SiO <sub>2</sub>	CO <sub>2</sub>	0-60	CO <sub>2</sub> /CH <sub>4</sub> (10-15)	2.00×10 <sup>-6</sup>	92
ZIF-69	7.8	$\alpha$ -Al <sub>2</sub> O <sub>3</sub> disks	CO <sub>2</sub>	RT	CO <sub>2</sub> /CO (3.5)	3.60×10 <sup>-8</sup>	44
ZIF-69	7.8	$\alpha$ -Al <sub>2</sub> O <sub>3</sub> disks	CO <sub>2</sub>	RT	CO <sub>2</sub> /N <sub>2</sub> (6.3) CO <sub>2</sub> /CO (5) CO <sub>2</sub> /CH <sub>4</sub> (4.6)	1.00×10 <sup>-7</sup>	93
SIM-1	8	$\alpha$ -Al <sub>2</sub> O <sub>3</sub> tube	CO <sub>2</sub> /N <sub>2</sub>	RT	CO <sub>2</sub> /N <sub>2</sub> (4.5)	8.00×10 <sup>-8</sup>	94
IRMOF-3	9.6	$\alpha$ -Al <sub>2</sub> O <sub>3</sub> disks	CO <sub>2</sub> /C <sub>3</sub> H <sub>8</sub>	RT	CO <sub>2</sub> /C <sub>3</sub> H <sub>8</sub> (~1.3*)	7.00×10 <sup>-7</sup>	95
IRMOF-3-AM6	9.6	$\alpha$ -Al <sub>2</sub> O <sub>3</sub> disks	C <sub>3</sub> H <sub>8</sub> /CO <sub>2</sub>	RT	C <sub>3</sub> H <sub>8</sub> /CO <sub>2</sub> (~2*)	5.00×10 <sup>-7</sup>	95
Bio-MOF-1	5.7 ~ 9.6	tubular porous stainless steel supports	CO <sub>2</sub>	RT	CO <sub>2</sub> /CH <sub>4</sub> (2.6)	1.10×10 <sup>-6</sup>	96

\* Idea separation factor, and  $\delta$  is the permeance of favoured molecules

**Table 3.** Summary of MOF membranes for other gases separation

MOF	Pore size (Å)	Substrate	Application	Temp. (°C)	Separation factor	Permeance (molm <sup>-2</sup> s <sup>-1</sup> Pa <sup>-1</sup> )	ref
ZIF-8	3.4	TiO <sub>2</sub> disks	Ethene/Ethane	RT	Ethene/Ethane (2.4)	1.70×10 <sup>-8δ</sup>	97
ZIF-8	3.4	α-Al <sub>2</sub> O <sub>3</sub> disks	propylene/propane	RT	propylene/propane (55)	2.00×10 <sup>-8</sup>	61
ZIF-8	3.4	α-Al <sub>2</sub> O <sub>3</sub> disks	propylene/propane	RT	propylene/propane (30)	7.00×10 <sup>-9</sup>	98
ZIF-8	3.4	α-Al <sub>2</sub> O <sub>3</sub> disks	propylene/propane	RT	propylene/propane (40)	2.00×10 <sup>-8</sup>	99
ZIF-8	3.4	α-Al <sub>2</sub> O <sub>3</sub> tube	propylene/propane	RT	propylene/propane (59)	2.50×10 <sup>-9</sup>	100
ZIF-8	3.4	α-Al <sub>2</sub> O <sub>3</sub> disks	propylene/propane	35	propylene/propane (30.1)	1.12×10 <sup>-8</sup>	101
ZIF-8	3.4	α-Al <sub>2</sub> O <sub>3</sub> disks	propylene/propane	-15-180	propylene/propane (50)	3.00×10 <sup>-8</sup>	102
ZIF-8	3.4	α-Al <sub>2</sub> O <sub>3</sub> disks	ethane/propane	RT	ethane/propane (80)	7.23×10 <sup>-8</sup>	103
ZIF-8	3.4		ethylene/propylene		ethylene/propylene (10)	1.47×10 <sup>-7</sup>	
ZIF-8	3.4		ethylene/propane		ethylene/propane (167)	1.50×10 <sup>-7</sup>	

$\delta$  is the permeance of favoured molecules

### 3. MOF Membranes for Separations

As the core of the membrane separation technique, a membrane's performance significantly influences the separation efficiency. MOF membranes have attracted increasing attention from researchers worldwide as a novel and promising material.<sup>104</sup> There are two main types of membrane materials based on the MOFs for separation. One is large-area polycrystalline, supported either by porous or free-standing substrates.<sup>37, 39, 41</sup> The other type mixes species to form a hybrid mixed matrix membrane (MMM).<sup>105</sup> This review focuses on the large-area polycrystalline, which comprises pure continuously grown MOFs. As discussed above, various methods and supports have been applied in the preparation of high-quality MOF membranes, and most were carried out for separation applications. Thus, we present the numbers of samples and development processes for MOF separation membranes. Different structures and pore sizes are required for different components, and this need for diversity gives the highly designable and flexible MOF materials an advantage. In the following section, many successful studies on different separation fields are discussed and in each case the background and requirements of application are illustrated – from gas to liquid separation.

#### 3.1 Gas separation

Polymer membranes are most commonly used for membrane - based gas separation in industries due to their low cost and ease of processing.<sup>9</sup> However, the economics of membrane processing is mainly determined by the selectivity and permeability. On the one hand, low selectivity results in multi-step separation processes with higher operative complexity and costs. On the other hand, smaller permeability may cause an increase in the use of membrane modules and low yield. A membrane with a suitable pore size capable of providing both high selectivity and permeability to a separation process are necessary for application. In the polymer membranes, it is difficult to simultaneously reach ideal permselectivity and flux values due to their disorder structures. In sharp contrast, zeolitic membranes with a uniform pore size can exhibit high performance in gas separation due to relatively fixed channels.<sup>106-109</sup> Coronas *et al.* has provided a comprehensive review of gas separation through zeolite membranes.<sup>110</sup> However, the chemical tailorability of zeolite membranes has limited their wider application for gas separation. The situation is quite different for the MOF materials, as their pore structures can be adjusted using a variety of easy methods. People can try

various MOFs to find ones suitable for the separation of gas molecules of different sizes. Numerous studies have been published in this area, and Tables 1-3 present most of the examples of MOF membranes corresponding to gas separation, which and were available to the authors when this manuscript was finalised (March 2014).

##### 3.1.1 H<sub>2</sub> purification and recycling

Hydrogen provides reliable, sustainable, environmental and climate-friendly energy that meets the world's energy requirements through a high energy density. Hydrogen is relevant to all of the energy sectors: transportation, buildings, utilities and industry,<sup>111</sup> unfortunately, it usually coexists with other light gases (CO<sub>2</sub>, CH<sub>4</sub>, N<sub>2</sub>, etc.) during production from industrial processes such as gasification or steam reforming reactions. To make better use of these hydrogen-rich streams as fuels, hydrogen must be separated from the mixtures. To achieve this goal of high-purity hydrogen, new technologies are needed. Those developed thus far have featured an integration of new materials, simplicity and economics. Nanoporous membranes, a branch of materials science, are expected to contribute in the coming transition from energy-cost systems (pressure swing adsorption or cryogenic separation) to a sustainable process.<sup>112</sup> Accordingly, zeolite membranes with well-defined pore structures have been prepared and investigated for refining hydrogen from exhausted gas streams.<sup>13</sup> Recently, MOF membranes - as a subclass of zeolitic materials - have been proposed and used for gas separation; specifically, hydrogen recovery. The H<sub>2</sub> purification and recycling properties of reported MOF membranes are summarised in Table 1.

In some pioneering works, famous and stable MOFs have been selected to prepare membranes for studying the permeation properties of H<sub>2</sub> and other gas molecules. In 2009, Lai *et al.* demonstrated the synthesis of continuous, well-intergrown MOF-5 membranes (Fig. 16) on porous supports using an *in situ* growth technique.<sup>33</sup> The membranes had good adhesion to the supports, which were strong enough to conduct gas permeation studies. The results showed that the diffusion of simple gases through an MOF-5 membrane mainly follows the Knudsen diffusion behaviour. H<sub>2</sub> molecules with a lighter molecular weight produce a better permeance. Then, the same group reported a preferentially oriented MOF-5 membrane fabricated using the microwave-induced rapid seeding of MOF-5 crystals on porous substrates and the subsequent solvothermal

secondary growth of the seed crystals.<sup>83</sup> This membrane was consistent with the previous report, as the pore size of MOF-5 was bigger than that of all of the tested gas molecules.

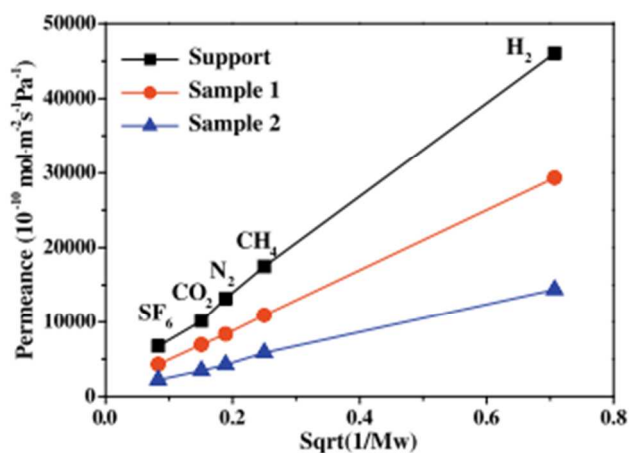


**Fig. 16** Single-component gas permeation results through the alumina support (square), sample 1 (circle) and sample 2 (triangle) under 800 Torr (Adapted with permission from ref.<sup>33</sup>).

HKUST-1(Cu<sub>3</sub>(BTC)<sub>2</sub>) is another classic MOF.<sup>113</sup> We have reported a work with this material using the ‘twin copper source’ method discussed in the last section.<sup>45</sup> The MOF of Cu<sub>3</sub>(BTC)<sub>2</sub> has an intersecting three-dimensional network containing large pores with a square cross-section (9 × 9 Å<sup>2</sup>), which is still larger than the common gas molecules. Although the sorption capacities of CO<sub>2</sub>, CH<sub>4</sub> and N<sub>2</sub> are much higher than that of H<sub>2</sub>, its reduced sorption correlates with the structural and chemical features of the present MOF, which favours the stronger interactions of CO<sub>2</sub>, CH<sub>4</sub> and N<sub>2</sub>. This selectivity of adsorption is helpful in the recycling of H<sub>2</sub> from other gases using the preferential adsorption mode. The effect of the mixed gas adsorption selectivity on the total membrane selectivity can be roughly estimated by the following simple relationship: ‘membrane selectivity = adsorption selectivity × diffusion selectivity’.<sup>91, 114</sup> In this case, the copper net-supported HKUST-1 membrane exhibited an excellent permeation selectivity for H<sub>2</sub> (H<sub>2</sub>/N<sub>2</sub> = 7, H<sub>2</sub>/CO<sub>2</sub> = 6.8 and H<sub>2</sub>/CH<sub>4</sub> = 5.9) and a high permeation flux (1 × 10<sup>-6</sup>) due to the superior porosity of HKUST-1 and the copper nets.

ZIF-8 – with the formula Zn(mim)<sub>2</sub> (mim = 2-methylimidazole), which crystallises with a sodalite-related structure – is highly stable but also shows adsorption affinity towards hydrogen and methane.<sup>115-117</sup> Given the narrow size of the six-membered-ring pores (~3.4 Å), a ZIF-8 membrane should be able to separate H<sub>2</sub> (kinetic diameter ~2.9 Å) from the larger molecules. The ZIF-8 membrane prepared in Caro’s work achieved a fine balance between flux (6.7 × 10<sup>-8</sup>) and selectivity (H<sub>2</sub>/CH<sub>4</sub> = 11.2) relative to other MOF membranes at that time.<sup>35</sup> It had the additional advantage of high thermal and chemical stability, which provided the possibility of increasing the permeance with steam. Furthermore, a thinner ZIF-8 membrane (1 μm) reported by Jeong *et al.* exhibited molecular sieving, which reflected ideal selectivities of 11.6 and 13 for H<sub>2</sub>/N<sub>2</sub> and H<sub>2</sub>/CH<sub>4</sub>, respectively.<sup>59</sup>

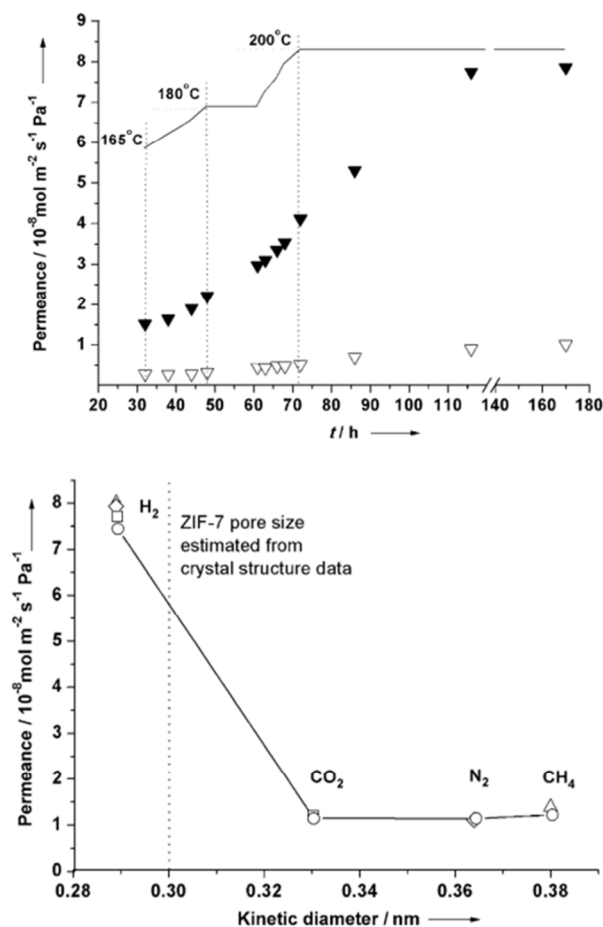


**Fig. 17** Top: H<sub>2</sub> (solid triangles) and N<sub>2</sub> (triangles) permeance from the 1:1 mixture through the ZIF-7 membrane during the on-stream activation process with increasing temperature. Bottom: Permeance of single gases (circles) and from 1:1 mixtures (squares: H<sub>2</sub>/CO<sub>2</sub> mixture, rhombuses: H<sub>2</sub>/N<sub>2</sub> mixture, triangles: H<sub>2</sub>/CH<sub>4</sub> mixture) of the ZIF-7 membrane at 200°C as a function of molecular kinetic diameters (Adapted with permission from ref.<sup>73</sup>).

The separation of MOF membranes is based on two concepts: preferential adsorption and shape selectivity. To separate H<sub>2</sub> from other gas molecules whose sizes are quite different, a suitable pore structure provides an ideal permselectivity. As a category of MOFs, ZIFs (zeolitic imidazolate frameworks) have emerged as a novel type of crystalline porous material for the preparation of superior molecular sieve membranes attributed to their zeolite-like properties, such as permanent porosity, uniform pore sizes and exceptional thermal and chemical stability.<sup>118-120</sup> These excellent performances have made ZIF membranes promising candidates for both hydrogen production and purification, even under high temperature conditions. Caro *et al.* have made ground-breaking advances in this area. They developed a series of supported ZIF membranes including SOD-type ZIF-7,<sup>73-75</sup> ZIF-8,<sup>35, 77</sup> ZIF-90,<sup>57, 70</sup> LTA-type ZIF-22<sup>58</sup> and a novel POZ topology porous ZIF-95.<sup>79</sup> Caro *et al.* also tested an ultramicroporous ZIF-7 for its gas-separation properties in membrane applications by synthesising it on a porous alumina support using a microwave-assisted

secondary growth technique.<sup>73</sup> This ZIF-7 membrane had several advantages: 1) its pore dimension approached the size of H<sub>2</sub>, so that a high H<sub>2</sub> selectivity could be obtained without any sophisticated pore-size engineering, which is essential for zeolite membranes targeting H<sub>2</sub>/CO<sub>2</sub> separation;<sup>121, 122</sup> 2) it was thermally stable for use at elevated temperatures; and 3) its hydrophobic property endowed it with very good hydrothermal stability. For applications at elevated temperatures, the activated ZIF-7 membrane was tested in single- and mixed-gas permeation at 200°C using the Wicke-Kallenbach technique and the results are partially collected in Fig. 17. The separation factors of the 1:1 binary mixtures (H<sub>2</sub>/N<sub>2</sub>, H<sub>2</sub>/CO<sub>2</sub> and H<sub>2</sub>/CH<sub>4</sub>) were 7.7, 6.5 and 5.9, respectively (at 200°C and 1 bar) – higher than the corresponding Knudsen separation factors. The results indicated a rather independent transport mechanism for the components of a mixture, which could be correlated with the ZIF-7 structure. ZIF-7 crystallised in the sodalite structure with a hexagonal arrangement of the cavities octahedrally interconnected by narrow windows interconnecting the cavities, which were responsible for the molecular sieving effect. The non-zero permeance of CO<sub>2</sub>, N<sub>2</sub> and CH<sub>4</sub> were attributed to the influence exercised by the non-size-selective mass transport through imperfect sealing or through the grain boundaries of the polycrystalline ZIF-7 layer.

Subsequently, ZIF-22 membranes with the same pore size as ZIF-7 (about 0.3 nm) were obtained by the same group using 3-aminopropyltriethoxysilane as a covalent linker to promote the nucleation and growth of ZIFs.<sup>58, 123</sup> For the ZIF-22 membranes, the mixture separation factors at 323 K of H<sub>2</sub>/CO<sub>2</sub>, H<sub>2</sub>/O<sub>2</sub>, H<sub>2</sub>/N<sub>2</sub> and H<sub>2</sub>/CH<sub>4</sub> were 7.2, 6.4, 6.4 and 5.2, respectively, with H<sub>2</sub> permeance higher than  $1.6 \times 10^{-7}$  molm<sup>-2</sup>s<sup>-1</sup>Pa<sup>-1</sup>. The H<sub>2</sub> permeance decreased slightly and the CO<sub>2</sub> permeance increased with increasing partial pressure, such that the H<sub>2</sub>/CO<sub>2</sub> selectivity decreased from 7.2 to 5.1 when the partial pressure increased from 0.5 to 1 bar.

Using the same linker, ZIF-90 membranes were prepared on the surface of an  $\alpha$ -Al<sub>2</sub>O<sub>3</sub> support by Caro *et al.*<sup>79</sup> The ZIF-90 membranes were thermally and hydrothermally stable and exhibited molecular sieve performance with a H<sub>2</sub>/CH<sub>4</sub> selectivity of more than 15. However, their H<sub>2</sub>/CO<sub>2</sub> selectivity was only 7.2 because their pore size (0.35 nm) was larger than the kinetic diameter of CO<sub>2</sub> (0.33 nm).<sup>124</sup> The separation of H<sub>2</sub> and CO<sub>2</sub> is important, such as through hydrogen production by the steam reforming of methane, including the water gas-shift strategy.<sup>125</sup> Caro *et al.* tried to improve the H<sub>2</sub>/CO<sub>2</sub> permselectivity of the ZIF-90 membranes by increasing the interaction between the CO<sub>2</sub> and the framework, which is schematised in Fig. 18. By applying the imine condensation reaction,<sup>126-128</sup> a novel covalent post-functionalization strategy was developed to modify the ZIF-90 membrane and enhance its hydrogen selectivity, which was helpful in eliminating invisible intercrystalline defects in the ZIF-90 layer, enhancing the molecular sieving performance.<sup>70</sup> Furthermore, the presence of the imine functionality in ZIF-90 can constrict the pore aperture, improving molecular sieving for the separation of H<sub>2</sub> from CO<sub>2</sub> and other large gases. Using covalent post-functionalization, the H<sub>2</sub>/CO<sub>2</sub> selectivity could be increased from 7.3 initially to 62.5 – a significant enhancement that suggested a method for reaching the target of high selectivity.

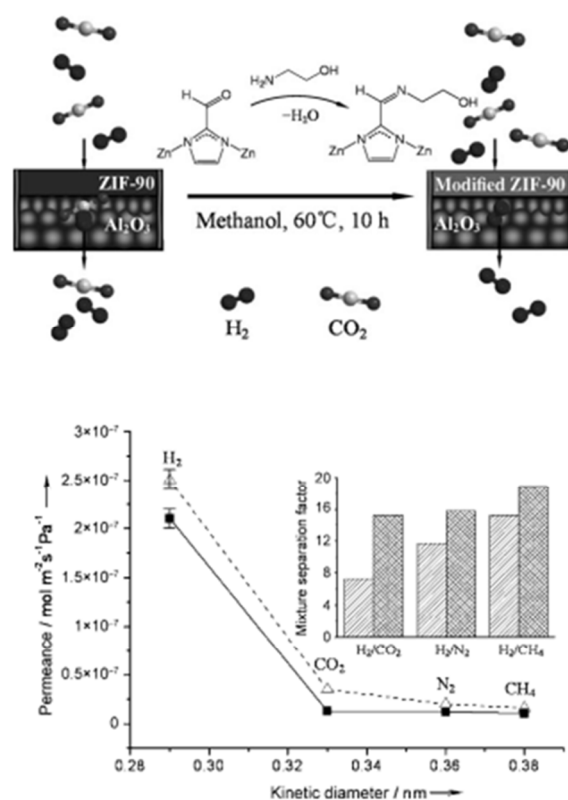


**Fig. 18** Top: Covalent post-functionalisation of a ZIF-90 molecular sieve membrane by imine condensation with ethanolamine to enhance H<sub>2</sub>/CO<sub>2</sub> selectivity. Bottom: Single-gas permeance on the as-prepared ( $\Delta$ ) and imine-functionalised ( $\blacksquare$ ) ZIF-90 membrane at 200°C and 1 Barrer (bar) as a function of the kinetic diameter (measured with a bubble counter). The inset shows the mixture separation factors for H<sub>2</sub> over other gases from equimolar mixture as determined by gas chromatography using the Wicke–Kallenbach technique before (hatched columns) and after (crossed columns) imine functionalisation (Adapted with permission from ref.<sup>70</sup>).

Due to the high stability associated with the MIL series, MIL-53 was also selected for membrane fabrication.<sup>129</sup> Jin *et al.* reported a well-intergrown MIL-53(Al) membrane obtained by a facile reactive seeding (RS) method.<sup>66</sup> The permeabilities of the small gas molecules indicated that the permeation behaviour mainly followed the Knudsen diffusion law. The channel size of the MIL-53 material ( $7.3 \times 7.7$  Å) was larger than the kinetic diameters of most of the small gas molecules, yet it fit the kinetic diameters of some of the liquid molecules, as discussed in the section on liquid separation.

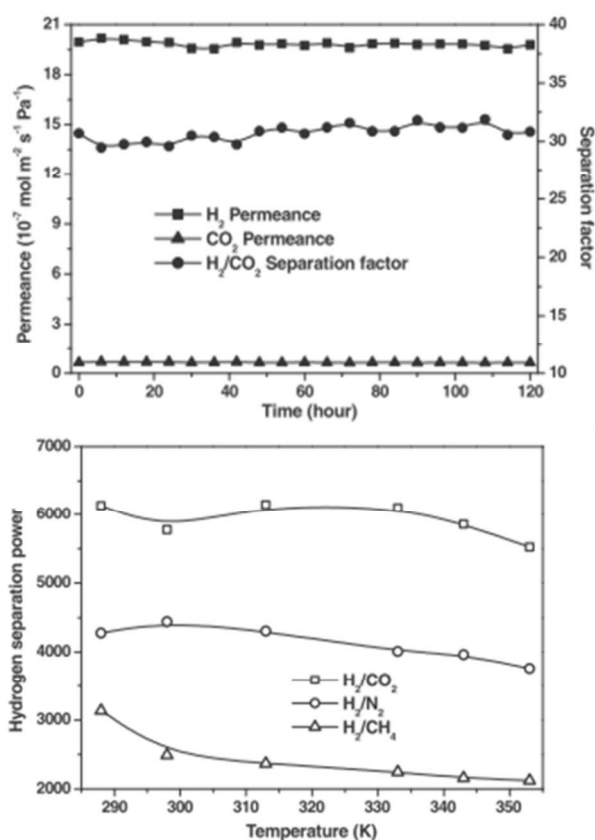


**Fig. 19** Top: Plot of H<sub>2</sub>/CO<sub>2</sub> permeance and separation factors for the NH<sub>2</sub>-MIL-53(Al) membrane versus test time. Bottom: Hydrogen separation power of the NH<sub>2</sub>-MIL-53(Al) membrane as a function of the permeation temperature (Adapted with permission from ref.<sup>63</sup>).

As we demonstrated in a previous study, the adsorption affinities of MOFs can be tuned by introducing functional groups that strongly interact with specific molecular species.<sup>63</sup> Continuous NH<sub>2</sub>-MIL-53(Al) membranes have been prepared successfully on macroporous glass frit discs, assisted by colloidal seeds. The adsorption results of this material have shown the preferred adsorption of specific gases, and the variations in the gas interactions with the NH<sub>2</sub>-MIL-53(Al) framework appear promising for gas separation applications.<sup>130</sup> As Fig. 19 shows, the membrane was highly selective for H<sub>2</sub> permeation with a separation factor higher than 20. The permeation behaviour of H<sub>2</sub>, CH<sub>4</sub>, N<sub>2</sub> and CO<sub>2</sub> through the membrane was investigated at different temperatures and a possible separation mechanism was discussed on the basis of sorption isotherms coupled with gas permeation measurements. In addition, as-prepared membranes have been proven to exhibit very high permeance for H<sub>2</sub>, together with very high hydrogen separation power. The supported NH<sub>2</sub>-MIL-53(Al) membranes have shown high stability and reproducibility, which are of potential interest in hydrogen gas recycling and recovery applications.<sup>131</sup>

In other work reported by our group, a stainless steel net-supported HKUST-1 membrane was prepared by polymer grafting, which produced better separation factors (H<sub>2</sub>/CO<sub>2</sub> = 9.24, H<sub>2</sub>/N<sub>2</sub> = 8.91 and H<sub>2</sub>/CH<sub>4</sub> = 11.2).<sup>60</sup> As Fig. 20 shows, we

also successfully fabricated a high-performance and continuous HKUST-1 membrane using a secondary growth approach on pre-seeded  $\alpha$ -Al<sub>2</sub>O<sub>3</sub> hollow ceramic fibres (HCFs) modified with chitosan.<sup>86</sup> The synthesised membrane showed high H<sub>2</sub> selectivity with separation factors of 8.66, 13.56 and 6.19 for the gas mixtures of H<sub>2</sub>/N<sub>2</sub>, H<sub>2</sub>/CO<sub>2</sub> and H<sub>2</sub>/CH<sub>4</sub>, respectively. A preferred permeance for H<sub>2</sub> in the binary gas mixture was obtained in the range of  $3.23 \times 10^{-8}$  to  $4.1 \times 10^{-8} \text{ mol m}^{-2} \text{ s}^{-1} \text{ Pa}^{-1}$ .

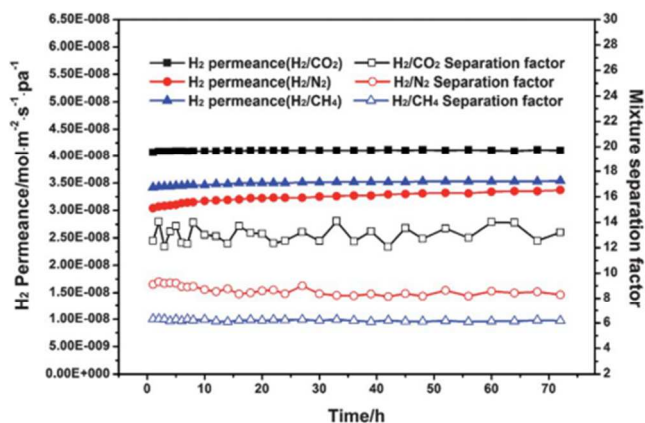


**Fig. 20** H<sub>2</sub> permeance and separation factors in the volume ratio 1:1 binary gas mixture H<sub>2</sub>/CO<sub>2</sub>, H<sub>2</sub>/N<sub>2</sub> and H<sub>2</sub>/CH<sub>4</sub> systems of Cu<sub>3</sub>(BTC)<sub>2</sub> membrane as a function of time at 40°C with a pressure drop of 1 atm (Adapted with permission from ref.<sup>86</sup>).

After developing a series of supported ZIF membranes, including ZIF-7, ZIF-8, ZIF-90 and ZIF-22, Caro *et al.* fabricated a ZIF-95 membrane with a novel POZ topology.<sup>79, 132</sup> This material was not only highly thermally stable up to 500°C but also exhibited permanent microporosity with constricted windows (~0.37 nm) and huge cavities (2.4 nm). In particular, ZIF-95 had a high affinity and capacity for CO<sub>2</sub> adsorption, making it promising for CO<sub>2</sub> capture. Given these properties, the strongly adsorbed component (CO<sub>2</sub>) is immobilised in the big cavities and permeation becomes diffusion-controlled in favour of the highly mobile component (H<sub>2</sub>). For mixed gas permeance and the H<sub>2</sub>/CO<sub>2</sub> selectivity at 1 bar, the H<sub>2</sub> permeance increased from  $5.00 \times 10^{-7}$  to  $1.96 \times 10^{-6} \text{ mol m}^{-2} \text{ s}^{-1} \text{ Pa}^{-1}$  and the CO<sub>2</sub> permeance slightly increased from  $5.91 \times 10^{-8}$  to  $7.64 \times 10^{-8} \text{ mol m}^{-2} \text{ s}^{-1} \text{ Pa}^{-1}$  as the temperature increased from 25°C to 325°C, resulting in an observable increase in the H<sub>2</sub>/CO<sub>2</sub> mixture separation factor from 8.5 to 25.7. This phenomenon can be explained by the preferential adsorption model. Given ZIF-95's high affinity and capacity for CO<sub>2</sub> adsorption, mainly CO<sub>2</sub> was adsorbed by the ZIF-95 pores at low temperatures (Fig. 21), which blocked the diffusion of the rarely adsorbed and highly mobile H<sub>2</sub>. As the temperature increased, less CO<sub>2</sub> was adsorbed and thus more H<sub>2</sub> could diffuse in the resulting free volume, significantly enhancing the H<sub>2</sub> permeance and selectivity.

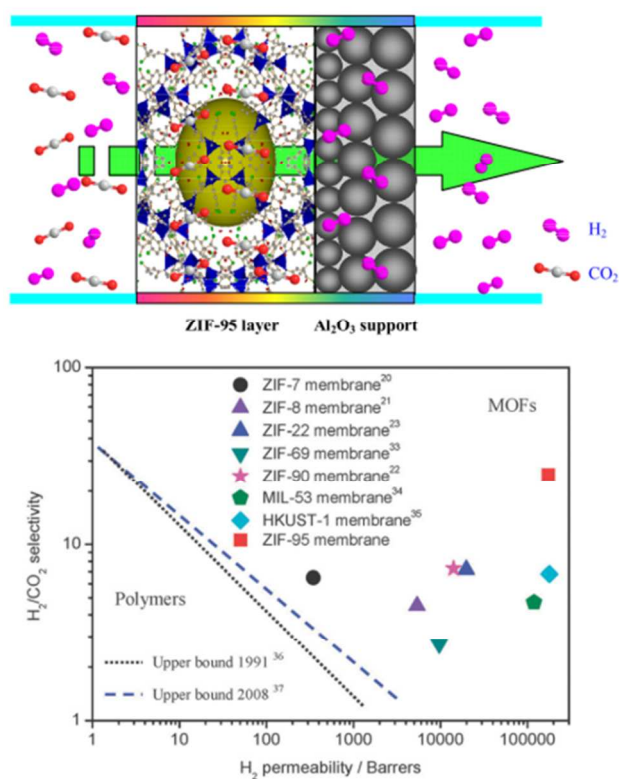


**Fig. 21** Top: Scheme for the fabrication of ZIF-95 molecular sieve membrane as carbon dioxide captor for H<sub>2</sub>/CO<sub>2</sub> separation. Bottom: H<sub>2</sub> /CO<sub>2</sub> selectivity versus H<sub>2</sub> permeability for polymeric and MOF membranes (Adapted with permission from ref.<sup>79</sup>).

In addition to ZIFs, some layer-pillar structures also provide tailored pore sizes by changing the pillars. For instance, Cu(bipy)<sub>2</sub>(SiF<sub>6</sub>), a MOF that represents a prototypical ‘pillared sheet’ platform that offers opportunities to control the pore sizes,<sup>133</sup> was initially reported as one of the best sorbents for CH<sub>4</sub> in 2000.<sup>134</sup> Recently, Eddaoudi and Zaworotko *et al.* developed a family of MOFs based on this framework, offering an unprecedented CO<sub>2</sub> sorption selectivity over N<sub>2</sub>, H<sub>2</sub> and CH<sub>4</sub>,<sup>4</sup> even in the presence of moisture. We successfully made this structure into a membrane for the H<sub>2</sub> purity, and the Cu(bipy)<sub>2</sub>(SiF<sub>6</sub>) membrane’s separation factors for H<sub>2</sub>/CO<sub>2</sub>, H<sub>2</sub>/CH<sub>4</sub> and H<sub>2</sub>/N<sub>2</sub> were 8.0, 7.5 and 6.8, respectively, at 293 K and 1 bar with an H<sub>2</sub> permeance of 2.7 × 10<sup>-7</sup> molm<sup>-2</sup>s<sup>-1</sup>Pa<sup>-1</sup> and high thermal stability. We expect to explore more Cu(bipy)<sub>2</sub>(SiF<sub>6</sub>) analogue membranes with tuneable pore sizes using this route, and to obtain membranes with better gas separation performance.<sup>89</sup>

Although efficient membranes with high selectivity and permeance have been reported, polycrystalline membranes of microporous materials have not fulfilled the principles of molecular design for microporous membranes. The results of defects and boundaries between individual crystals in polycrystalline membranes, which also result in the low reproducibility of experimental data, prevent the precise estimation of gas permeation, especially for small-molecule gases such as H<sub>2</sub>, He and CO<sub>2</sub>. One of the most reliable methods for studying gas permeation is the use of single-crystal

membranes. Takamizawa *et al.* reported a porous single crystal of the metal complex [Cu<sub>2</sub>(bza)<sub>4</sub>(pyz)]<sub>n</sub><sup>72</sup> that is easily obtained as well-formed single crystals to act as a single-crystal membrane. The single-crystal membrane exhibited gas permeability along and barrier properties perpendicular to the channel direction. Permeability values along the channels (channel membrane) were 7-60 times greater than those perpendicular to the channels (nonchannel membrane) for corresponding gases. The permeability perpendicular to the channels was undetectable for N<sub>2</sub>, Ar, CO, O<sub>2</sub> and CH<sub>4</sub> gases under the measurement conditions. He, H<sub>2</sub> and CO<sub>2</sub> gases permeated slightly perpendicular to the channels, probably due to a small number of crystal defects for the H<sub>2</sub> and He gases and the high adsorption ability of CO<sub>2</sub> gas. This clearly indicated that the gases permeated the membrane through the channels, even though the channel neck diameter (~2Å) was smaller than the kinetic diameters of the sample gases (2.55-3.80Å). For the H<sub>2</sub> and CO<sub>2</sub> gas permeation, the experimental permeability was much faster than the calculated permeability, indicating that easy gas permeation through the narrow channels was supported by the structural flexibility of [Cu<sub>2</sub>(bza)<sub>4</sub>(pyz)]<sub>n</sub>. This suggested that flexible ultramicroporous materials have great potential in the development of membranes as crystal devices in gas purification techniques.

### 3.1.2 CO<sub>2</sub> separation

Natural gas used as fuel shows outstanding advantages, including high storage ability, high energy content and clean post-combustion products. It has become one of the fastest growing primary energy sources in the world today.<sup>135, 136</sup> The increasing global demand for energy has required the increased production of high-quality natural gas. On the one hand, carbon dioxide is one of the major contaminants of natural gas and must be removed (controlled) to meet the required specifications before the gas is delivered to the pipeline. On the other hand, the purification and recovery of CO<sub>2</sub> from natural or flue gas are of great interest for energy production and from the conservation perspective. Additionally, CO<sub>2</sub> is the major greenhouse gas, and its accumulation triggers severe global warming issues. Thus, it is urgent to separate and recycle CO<sub>2</sub>.<sup>137, 138</sup> Membrane technology is a promising and attractive alternative to the conventional processes, as it offers more energy efficiency and excellent reliability. The removal of CO<sub>2</sub> without large energy expenditure is particularly desirable. Therefore, many membranes have been developed for CO<sub>2</sub> separation. In the past few decades, polymer membranes have become well known and widely used in gas separation owing to their relatively low cost and ease of processing.<sup>139, 140</sup> However, plasticisation could significantly decrease their performance and alter their permeability and selectivity, as Robeson showed. To go beyond the limits of polymer membranes, new materials must be developed. Consequently, inorganic zeolite-based membranes have been extensively studied during the past decade. Zeolites have superior thermal, mechanical, chemical and high-pressure stability than their polymer counterparts. Zeolite membranes, such as the FAU,<sup>141</sup> DDR,<sup>142</sup> ERI,<sup>143</sup> CHA<sup>138, 144, 145</sup> and MFI<sup>12, 146</sup> types have been used for CO<sub>2</sub>/CH<sub>4</sub> separation. Although these membranes have demonstrated high selectivity for CO<sub>2</sub> over CH<sub>4</sub>, some of them have low permeability driven by a high pressure drop.

Due to ZIF-8’s highly porous open framework structure, large accessible pore volume with fully exposed edges and organic link faces, pore apertures within the range of several gas

molecules' kinetic diameters and high CO<sub>2</sub> adsorption capacity, it has become highly attractive for use in gas separation applications. Furthermore, it has been demonstrated that ZIF-8 is chemically stable in the presence of water and some aromatic hydrocarbons such as benzene, which are typical impurities in natural gas, making this particular ZIFs composition potentially useful for separating CO<sub>2</sub> from CH<sub>4</sub>.<sup>118</sup> As Carreon *et al.* reported, ZIF-8 membranes were synthesised by *in situ* crystallisation on tubular porous  $\alpha$ -alumina supports, with hydrothermal synthesised seeds providing nucleation sites for membrane growth.<sup>96</sup> And all of the membranes were coated with two layers except one (Z4), which was coated with eight layers. The thickness of the two-layer membranes was  $\sim 5 \mu\text{m}$  and the eight-layer membrane was  $\sim 9 \mu\text{m}$  thick. The small thickness difference between the two- and eight-layered membranes suggested partial dissolution of the first layers. ZIF-8 crystals of  $\sim 110 \pm 15 \text{ nm}$  allowed the formation of continuous thin membranes. ZIF-8 membranes displayed unprecedented high CO<sub>2</sub> permeance up to  $\sim 2.4 \times 10^{-5} \text{ molm}^{-2}\text{s}^{-1}\text{Pa}^{-1}$  and CO<sub>2</sub>/CH<sub>4</sub> selectivity from  $\sim 4$  to 7 at 295K and a feed pressure of 139.5 KPa – the maximum pressure the membranes could hold. Although ZIF-8 is composed of large 11.6 Å pores and small pore apertures of 3.4 Å, density functional theory simulation data suggested that the smaller pores were the preferential adsorption sites for CO<sub>2</sub> molecules. Therefore, the small pore aperture of ZIF-8 may favour the diffusion of CO<sub>2</sub> (kinetic diameter  $\approx 3.3 \text{ \AA}$ ) over CH<sub>4</sub> (kinetic diameter  $\approx 3.8 \text{ \AA}$ ).

membrane as a function of test time (Adapted with permission from ref.<sup>92</sup>).

Because the molecular sizes of CH<sub>4</sub> and CO<sub>2</sub> are quite similar, it is difficult to achieve their separation through shape selectivity in a membrane process. With their composition of varied metal ions and organic ligands, MOFs have exhibited the selective adsorption of these two gases, providing hope that they might be used to separate CO<sub>2</sub> from CH<sub>4</sub> through a preferential adsorption mode. For instance, we reported continuous intergrown layers of Co<sub>3</sub>(HCOO)<sub>6</sub> on a macroporous glass frit using a secondary-growth method, which we used as membranes.<sup>92</sup> The microporous Co<sub>3</sub>(HCOO)<sub>6</sub> material exhibited high thermal stability and diamondoid connectivity, and the overall framework gave rise to one-dimensional zigzag channels with an effective pore size of 5.5 Å. This channel system was appropriate for CO<sub>2</sub> separation from CH<sub>4</sub>. The separation behaviour and the possible separation mechanism were deduced on the basis of sorption isotherms of CO<sub>2</sub> and CH<sub>4</sub> combined with *in situ* IR measurements. As the permeance shows in Fig. 22, the microporous glass-frit-supported Co<sub>3</sub>(HCOO)<sub>6</sub> membrane exhibited a high permeation flux (as high as  $2.09 \times 10^{-6} \text{ molm}^{-2}\text{s}^{-1}\text{Pa}^{-1}$ ) and excellent permeation selectivity for CO<sub>2</sub> over CH<sub>4</sub> (in the range of 10.37–15.95) at 0°C–60°C. The CO<sub>2</sub> molecules passed more easily through the zigzag channels of the MOF membrane than did the bulkier CH<sub>4</sub> molecules. This result was a consequence of the preferential adsorption of CO<sub>2</sub> in the micropores and at the external surfaces of the Co<sub>3</sub>(HCOO)<sub>6</sub> membrane, which inhibited CH<sub>4</sub> sorption from the mixture when a stable separation process was attained. The effective pore size of the Co<sub>3</sub>(HCOO)<sub>6</sub> membrane (5.5 Å) combined with the pore shape did not allow two molecules to pass through simultaneously, such that once the CO<sub>2</sub> was diffusing through the pores, the diffusion of CH<sub>4</sub> molecules was blocked.

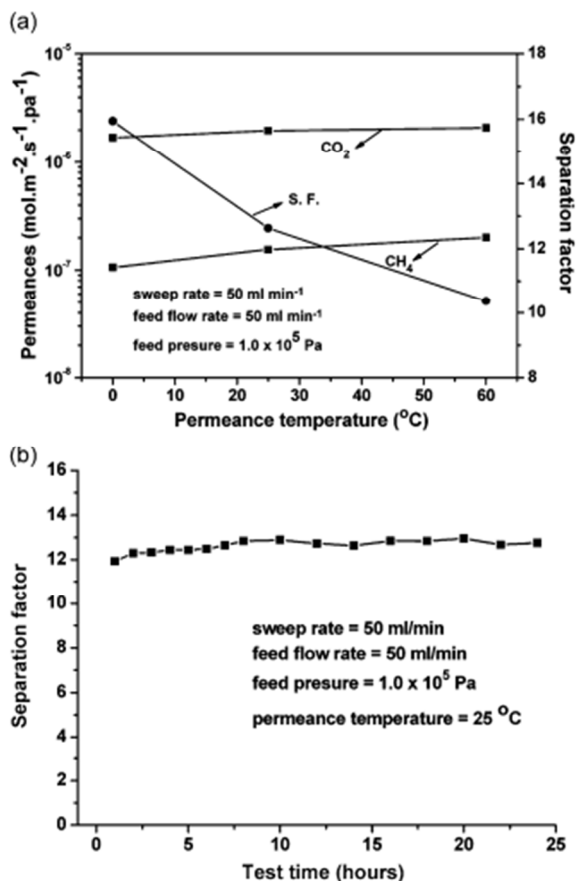


**Fig. 22** a) CO<sub>2</sub>/CH<sub>4</sub> permeance and separation factor (SF) of the Co<sub>3</sub>(HCOO)<sub>6</sub> membrane versus permeation temperature. b) Plot of the CO<sub>2</sub>/CH<sub>4</sub> separation factor of the Co<sub>3</sub>(HCOO)<sub>6</sub>

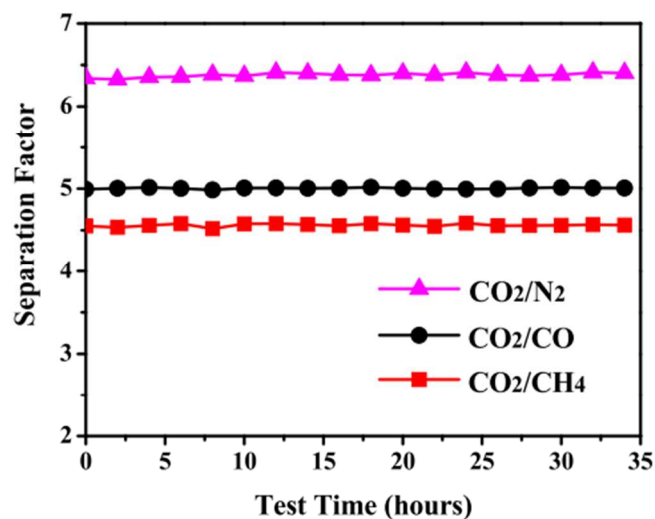


**Fig. 23** Separation factors for the CO<sub>2</sub>/CO, CO<sub>2</sub>/CH<sub>4</sub> and CO<sub>2</sub>/N<sub>2</sub> gas mixtures (50% molar each) as a function of test time for ZIF-99 membrane at 298 K (Adapted with permission from ref.<sup>93</sup>).

In the separation process based on the zeolites, the oriented membranes produced some remarkable results.<sup>6, 10</sup> Similarly, some successful stories with highly oriented MOFs were also reported for gas separation and other applications.<sup>23, 75, 83, 91, 147</sup> The ZIF-69 membrane possessed a zeolite GME topology with 12 membered ring (MR) straight channels along the *c*-axis and 8 MR channels along the *a*- and *b*-axes. The pore size along the *c*-axis was about 0.78 nm.<sup>148</sup> According to Lai *et al.*, to achieve better gas permeation performance, one would expect the optimal microstructure of ZIF-69 membranes to be thin, compact and most importantly *c*-oriented; that is, all of the straight channels aligned perpendicular to the support surface. They obtained this membrane using a second growth method with oriented seeds.<sup>93</sup> The single-gas permeation experiments indicated that N<sub>2</sub>, CO and CH<sub>4</sub> mainly followed the Knudsen diffusion mechanism, whereas CO<sub>2</sub> was dominated by surface diffusion due to the adsorption affinity of ZIF-69. The separations of the equimolar mixture gases CO<sub>2</sub>/N<sub>2</sub>, CO<sub>2</sub>/CO and CO<sub>2</sub>/CH<sub>4</sub> – studied in the Wicke-Kallenbach mode and measured by gas chromatograph (GC) – were 6.3, 5.0 and 4.6, respectively, with a permeance of  $\sim 1.0 \times 10^{-7}$  mol m<sup>-2</sup> s<sup>-1</sup> Pa<sup>-1</sup> for CO<sub>2</sub> at room temperature (Fig. 23). Compared to ZIF-69 membranes synthesised by the *in situ* crystallisation methods,<sup>44</sup> the highly *c*-oriented ZIF-69 membrane exhibited better selectivity and higher permeance.

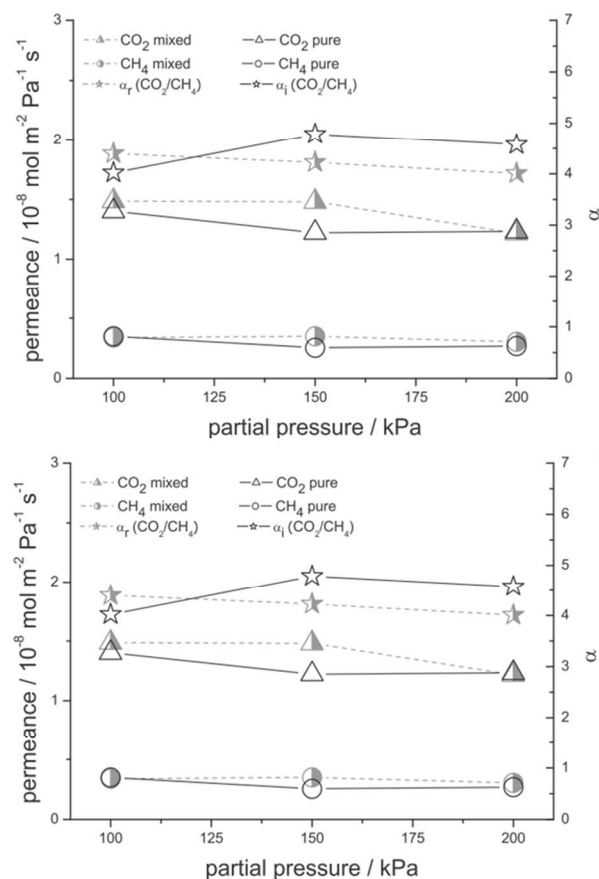


**Fig. 24** Top: Permeance of pure and equimolar mixed CO<sub>2</sub> and CH<sub>4</sub> measured for the [Cu<sub>2</sub>(ndc)<sub>2</sub>(dabco)]<sub>n</sub> (1) membrane at room temperature (T = 298K) as function of pressures at the feed side (total pressures for pure gases, partial pressures for the gas mixture). The ideal and mixed gas separation factors  $\alpha_i$  and  $\alpha_r$  were calculated

from the corresponding ratio of the CO<sub>2</sub>/CH<sub>4</sub> permeance. Bottom: Permeance of pure and equimolar mixed CO<sub>2</sub> and CH<sub>4</sub> measured for the [Cu<sub>2</sub>(BME-bdc)<sub>2</sub>(dabco)]<sub>n</sub> (2) membrane at room temperature (T=298K) as function of pressures at the feed side (total pressures for pure gases, partial pressures for the gas mixture). The ideal and mixed gas separation factors  $\alpha_i$  and  $\alpha_r$  were calculated from the corresponding ratio of the CO<sub>2</sub>/CH<sub>4</sub> permeance (Adapted with permission from ref.<sup>91</sup>).

In another work, Caro *et al.* reported on the first MOF membranes fabricated by stepwise liquid-phase deposition and evaluated their performance in mixed gas separation.<sup>91</sup> The preparation method was versatile and offered straightforward scale-up and automatization possibilities. The separation-active MOF layer was located inside the macroporous support in a depth ranging along the  $\mu$ m scale. The microstructures of the MOF-based membranes resembled foam, with the intergrown lamellae as a transport-selective membrane. Fig. 24 provides proof that the functionalization of linkers can induce CO<sub>2</sub> membrane selectivity. CO<sub>2</sub>/CH<sub>4</sub> mixtures were separated with an anti-Knudsen separation factor of 4-5 in favour of CO<sub>2</sub>. The isoreticular concept of MOFs can be used to derive membranes that show the adsorption-based rather than molecular sieve separation of gas mixtures.

### 3.1.3 Propylene/propane

Due to their close physical properties, olefin/paraffin separation (such as propylene/propane) is quite challenging,<sup>9</sup> yet commercially very important. Olefin/paraffin mixtures are traditionally separated using highly energy-intensive cryogenic distillation. Membranes have therefore gained tremendous interest as an energy-efficient alternative technology. It has been proposed that for membranes to be commercially viable, a minimum propylene permeability of 1 bar and a propylene selectivity of 35 are required. Thus far, many different types of membranes have been studied including polymer,<sup>149</sup> zeolite,<sup>150</sup> carbon molecular sieve,<sup>151</sup> mixed matrix<sup>152</sup> and facilitated transport.<sup>153</sup> However, most of these membranes suffer from limitations of one kind or another. For example, most polymeric membranes do not meet the selectivity/permeability threshold, as they suffer from low reliability and durability. The selectivity/permeability performance targets are also not met by more robust membranes such as zeolites and ceramics, or by mixed matrix membranes comprising highly selective phases that were dispersed in polymer matrix until recently. Facilitated transport membranes can be easily poisoned by a small amount of impurities, and carbon molecular sieve membranes are brittle, which makes it difficult to scale-up the production. Accordingly, it is evident that new material paradigms are essential to successfully address this energy-intensive yet industrially important separation. With unprecedented control over pore size and chemical/physical properties via a judicious choice of organic linkers, MOFs offer unique opportunities to overcome the limitations of not only current membrane materials, but also conventional membrane system design/integration and operation.

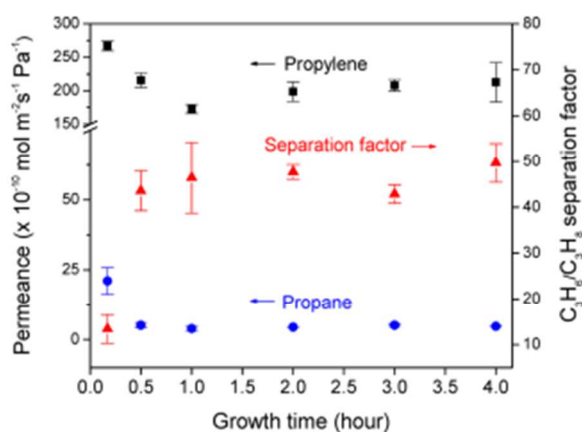


**Fig. 25** Propylene/propane separation performance of ZIF-8 membranes as a function of growth time at room temperature. ZIF-8 membranes show excellent propylene/propane separation factors ( $\sim 50$ ) even after growing for 30 min (Adapted with permission from ref.<sup>61</sup>).

The temperature dependences of both the single and binary propylene/propane separation performances of the propylene membranes decreased while those of the propane increased slightly as the temperature rose, which is consistent with the previous report in 2012.<sup>102</sup> This led to a decrease in the propylene/propane separation factor and ideal selectivity as the temperature increased. These trends can be explained by the surface diffusion model, in which the diffusion through microporous materials is described as an activation process involving the adsorption and subsequent diffusion of molecules by hopping along the adsorbent surface.<sup>154</sup> Therefore, the permeance of gas molecules depends on both the heat of adsorption and the activation energy for gas diffusion (i.e.,  $P \sim \exp(-(\Delta H_{\text{ads}} - E_a)/RT)$ ). The heats of the adsorption of propylene and propane on ZIF-8 were 30 and 34 kJ/mol, respectively, and the diffusional activation energies for propylene and propane were 9.7 and 74 kJ/mol, respectively.<sup>155</sup> As the temperature increased, the permeance of the propylene decreased while that of the propane increased. Furthermore, the ZIF-8 membranes were found to be mechanically strong with their separation performance maintained at a high level even after 2 h of intensive sonication.

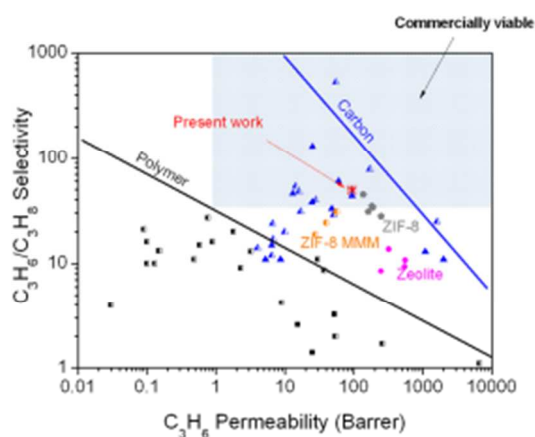


**Fig. 26** Comparison of the propylene/propane separation performance of our ZIF-8 membranes with those of other membranes reported in the literature. Half- and full-filled symbols indicate separation data from single and binary gas permeation measurements, respectively. The shaded area in the graph implies the performance requirement of a membrane (a minimum permeability of 1 bar and a selectivity of 35) for commercial application. The solid lines are the so-called Robison upper bound, the Triangle is the carbon membrane, the circle is a zeolite membrane, the rectangle is a polymer membrane, the pentagon is a ZIF-8 membrane, the hexagon is a ZIF-8 mixed matrix membrane the star is the ZIF-8 membrane in this work. Copyright 2013, American Chemical Society (Adapted with permission from ref.<sup>61</sup>).

Jeong *et al.* developed a one-step *in situ* synthesis technique for high-quality MOF membranes based on the concept of counter diffusion.<sup>61</sup> This simple yet highly versatile method enabled the rapid preparation of well-intergrown ZIF-8 membranes with excellent microstructures. The high-quality ZIF-8 membranes exhibited good separation performance when applied to a propylene/propane (50/50) mixture (selectivity  $\sim 55$ ). Fig. 25 shows the room-temperature propylene/propane separation performance of ZIF-8 membranes prepared for varying membrane growth times. Membranes grown even for 10 min started to show a moderate separation factor ( $\sim 3$ ). As the membranes were grown for longer times, the separation factor increased and then reached a plateau (55). Compared with the other membranes reported in the literature (Fig. 26), the aforementioned ZIF-8 membranes notably outperformed both the polymeric and zeolite membranes with respect to the separation factor and the propylene permeability. Furthermore, the membranes were close to the upper bound of carbon membranes while meeting the proposed requirements.

Jeong *et al.* also reported the preparation of ZIF-8 membranes for propylene/propane using several other methods. For instance, they used a novel strategy – rapid thermal deposition (RTD) – to quickly synthesise high-quality ZIF-8 membranes.<sup>98</sup> The propylene/propane selectivity on these membranes was  $\sim 30$ . Then, they applied a rapid and simple microwave-assisted seeding technique for the synthesis of high-quality ZIF-8 membranes.<sup>99</sup> The gas separation performance of the ZIF-8 membranes indicated that the membranes grown at 8°C showed an average propylene permeance of about 208 molPa<sup>-1</sup>m<sup>2</sup>s<sup>-1</sup> with an average propylene/propane separation factor of  $\sim 40$ . The separation performances (propylene permeance and separation factor) were enhanced as the growth temperature decreased. Their reasoning was that slow crystal growth at lower temperatures resulted in membranes with thinner thicknesses given the same growth time, and better grain boundary structure than the ones formed at higher temperatures.

In a recent work reported by Hara,<sup>100</sup> the contribution of the diffusive separation of propylene/propane was determined from the permeation properties of ZIF-8 membranes. These membranes were prepared using a counter diffusion method that resulted in the formation of an 80  $\mu\text{m}$ -thick ZIF-8 layer on the outermost section of a porous  $\alpha$ -alumina capillary substrate. Single-component gas permeation properties were investigated using helium, hydrogen, carbon dioxide, oxygen, nitrogen, methane, propylene and propane at temperatures ranging from 298 to 363 K. The molecular sieve gas permeation properties of the ZIF-8 membranes increased with the reaction time, which is consistent with the evolution of ZIF-8 crystal formation. The ZIF-8 membrane permeance of hydrogen and propylene reached  $9.1 \times 10^{-8}$  and  $2.5 \times 10^{-9}$  molm<sup>-2</sup>s<sup>-1</sup>Pa<sup>-1</sup>, respectively. The ideal separation factors for hydrogen/propane and propylene/propane at 298 K were found to be 2000 and 59, respectively. The diffusion separation factor increased with the

**Table 4.** Collection of MOF membranes for liquid separation

MOF	Pore size(Å)	Substrate	Method	Temp. (°C)	Separation factor	Flux (molm <sup>-2</sup> h <sup>-1</sup> )	Ref.
Ni <sub>2</sub> (L-asp) <sub>2</sub> bipy	2.8×4.7	α-Al <sub>2</sub> O <sub>3</sub> disks	Secondary growth	30	R-MPD/S-MPD ( <i>ee</i> %=35.5%)	1.5×10 <sup>-3 δ</sup>	156
Ni <sub>2</sub> (L-asp) <sub>2</sub> bipy	2.8×4.7	Nickel net	Single nickel source	25-200	R-MPD/S-MPD ( <i>ee</i> %=32.5%)	8.8	46
Zn <sub>2</sub> (cam) <sub>2</sub> (dabco)	3×3.5	QCM substrate	Layer by layer	RT	R-HDO/S-HDO ( <i>ee</i> %=21.6%)	-	157
ZIF-8	3.4	α-Al <sub>2</sub> O <sub>3</sub>	Secondary growth	RT	n-hexane/benzene (23*)	5.04	158
ZIF-8	3.4	PMPS	MMMs	RT	isobutanol/H <sub>2</sub> O (44)	61	71
ZIF-71	4.8	Porous ZnO	Secondary growth (reactive seeding)	RT	EtOH/water (6.07) MeOH/water (21.38) DMC/MeOH (5.34)	7 12 3	159
Zn <sub>2</sub> (bdc)(L-lac)(dmf)	5	Porous ZnO	Secondary growth (reactive seeding)	RT	R-MPS/S-MPS (33%)	1.5×10 <sup>-4</sup>	160
ZIF-78	7.1	Porous SiO <sub>2</sub>	Secondary growth	RT	cyclohexanol/cyclohexanone (2)	0.58	161
MIL-53(Al)	7.3×7.7	α-Al <sub>2</sub> O <sub>3</sub> disks	Secondary growth (reactive seeding)	60	water/ethyl acetate (>100)	25	66
Zn <sub>2</sub> (bdc) <sub>2</sub> dabco	7.5	Porous SiO <sub>2</sub>	Secondary growth	25-200	m-x/p-x (1.934) o-x/p-x (1.617)	19	162

<sup>δ</sup> The permeance of favoured molecules and \* Idea separation factor

decreasing temperature, reaching 23, whereas the solution separation factor remained 2.7. Therefore, the separation of propylene/propane was attributed to be mainly governed by diffusive separation.

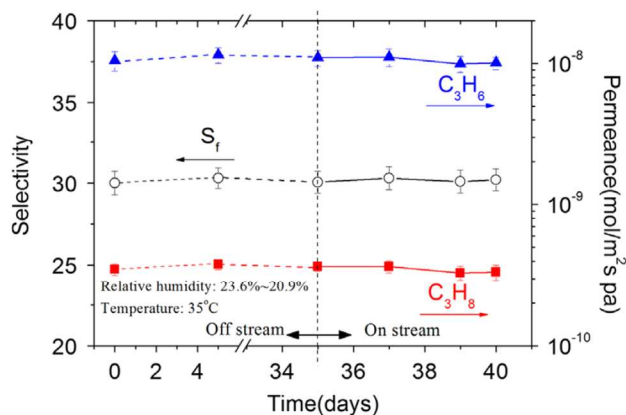


Fig. 27 Off-stream stability and on stream stability test of C<sub>3</sub>H<sub>6</sub>/C<sub>3</sub>H<sub>8</sub> mixture gases permeances on ZIF-8 membrane at 35 °C (Adapted with permission from ref.<sup>101</sup>)

Lin *et al.* also studied propylene/propane separation on high-quality ZIF-8 membranes prepared on the α-Al<sub>2</sub>O<sub>3</sub> support by secondary growth synthesis in water solution.<sup>101</sup> Single He, H<sub>2</sub>, CO<sub>2</sub>, N<sub>2</sub>, CH<sub>4</sub>, C<sub>3</sub>H<sub>6</sub> and C<sub>3</sub>H<sub>8</sub> permeation data for the ZIF-8 membranes were measured and analysed using a permeation model to obtain the gasses diffusivity values in ZIF-8 crystals. Gas permeance for the abovementioned light gases remained constant, whereas for C<sub>3</sub>H<sub>6</sub> and C<sub>3</sub>H<sub>8</sub> permeance decreased with the increasing pressure due to

the specific pressure dependencies of the adsorption isotherms respective to each gas. The determined diffusivities for propylene and propane were 1.25×10<sup>-8</sup> cm<sup>2</sup>/s and 3.99×10<sup>-10</sup> cm<sup>2</sup>/s with activation energies for diffusion of 12.7 kJ/mol and 38.8 kJ/mol, respectively. With an equal-molar binary feed, the ZIF-8 membranes exhibited a consistent C<sub>3</sub>H<sub>6</sub>/C<sub>3</sub>H<sub>8</sub> selectivity of about 30 and C<sub>3</sub>H<sub>6</sub> permeance of 1.1×10<sup>-8</sup> mol/m<sup>2</sup>sPa (Fig. 27). Both the permeance and selectivity decreased with the increasing feed pressure and the C<sub>3</sub>H<sub>6</sub>/C<sub>3</sub>H<sub>8</sub> selectivity decreased with the increasing temperature. A month-long stability test revealed the stable gas permeance and separation performance of the ZIF-8 membranes in both atmospheric conditions and the C<sub>3</sub>H<sub>6</sub>/C<sub>3</sub>H<sub>8</sub> mixture stream.

### 3.2 Liquid separation

It is difficult and uneconomical to transform some high-boiling liquid mixtures into gas phase for separation. However, such a transformation is crucial in some liquid separation applications such as chemical crude product, isomer separation and water removal. For these separations, the traditional methods are distillation, fluidised bed and adsorption – all of which require high energy consumption and large equipment that render the process environmentally unfriendly. As a novel and effective technique, membrane separation has proven promising in this field, yet chemical stability problems limit the application of polymer in liquid separation, especially in the organic mixtures. Zeolites have been investigated for some processes involving inorganic microporous membranes. For instance, Wang *et al.* reported an LTA-type zeolite membrane used to remove water from ethanol with an ideal selectivity.<sup>163</sup> Tsapatsis *et al.* also reported remarkable work on the separation of xylene isomers using

oriented MFI-type zeolite membranes.<sup>10</sup> However, zeolites' limited structures have kept them from being used in wider fields. MOFs are created by linking inorganic and organic units. The flexibility with which the constituents' geometry, size and functionality can be varied has led to more than 20,000 different MOFs being reported and studied within the past decade.<sup>104</sup> These thriving frameworks have great potential for liquid separation applications. Some of the pioneering research in this area is collected in Table 4.

### 3.2.1 Chiral resolution

Considerable attention is being paid to chiral resolution based on significant differences in the biological and pharmacological properties of the isomers of chiral compounds;<sup>164, 165</sup> that is, one has the desired affect while the other may be inert or even harmful. The optical resolution of racemic mixtures is possible through various separation techniques, including thin-layer chromatography (TLC), gas chromatography (GC), high performance liquid chromatography (HPLC), etc. However, all of these methods suffer from drawbacks such as small separation amounts per run, batch processing and high cost. As an alternative method, membrane separation's advantages such as low-energy consumption, large processing capacity and a continuous mode of operation allow it to dominate traditional methods. Some liquid and polymer membranes have been used for the optical resolution of chiral isomers. Although liquid membranes have demonstrated reasonably good permeability and enantioselectivity, they exhibit inferior durability and stability. Likewise, polymer membranes have some disadvantages such as a flexible skeleton and poor thermal stability that restrict their application in the field of chiral separation. Zeolites and mesoporous membranes have attracted intense interest due to their well-defined porosity and stability in engineering applications such as gas or liquid separation, membrane reactors and chemical sensors.<sup>10, 12, 166, 167</sup> However, it is very difficult to synthesize these materials with chiral structures, and such synthesis is the core of chiral separation. Therefore, exploring new types of membranes for application in chiral resolution is of critical importance. Chiral separation by inorganic membranes remains a challenging task, but it could be potentially achieved by MOF membranes because a chiral pore structure can be relatively easily prepared in MOFs by selecting the chiral ligand with the expected length and functional groups.

The enantiomeric SURMOFs  $[\text{Zn}_2(+)\text{cam}]_2(\text{dabco})_n$  and  $[\text{Zn}_2(-)\text{cam}]_2(\text{dabco})_n$  were synthesised directly on the SAM/Au-modified QCM substrate by Fischer *et al.*,<sup>157</sup> and these samples enabled the adsorption kinetics of enantiomers to be monitored and characterised. The differences in the absolute uptake and adsorption rates for each of the chosen enantiomeric probe molecules (2R,5R)-2,5-hexanediol (R-HDO) and (2S,5S)-2,5-hexanediol (S-HDO) were clear, indicating significant enantioselectivity. The results suggested that  $[\text{Zn}_2(+)\text{cam}]_2(\text{dabco})_n$  showed a roughly 1.5-fold preference for adsorption of R-HDO over S-HDO, whereas  $[\text{Zn}_2(-)\text{cam}]_2(\text{dabco})_n$  exhibited the inverted selectivity, a 1.5-fold adsorption of S-HDO over R-HDO. This very significant difference was attributed to the different interactions of R- and S-HDO with SURMOF containing (+) and (-) forms of camphorate. The QCM adsorption profiles are presented in Fig. 28. Because QCM cannot distinguish R- from S-HDO by the mass uptake only, the data on racemate separation could not be gained using this approach. The SURMOFs grown on QCM substrates as described in this work may serve as valuable devices for (high throughput) automatic screening MOFs and analytes to optimise enantioselectivity in chiral separations.

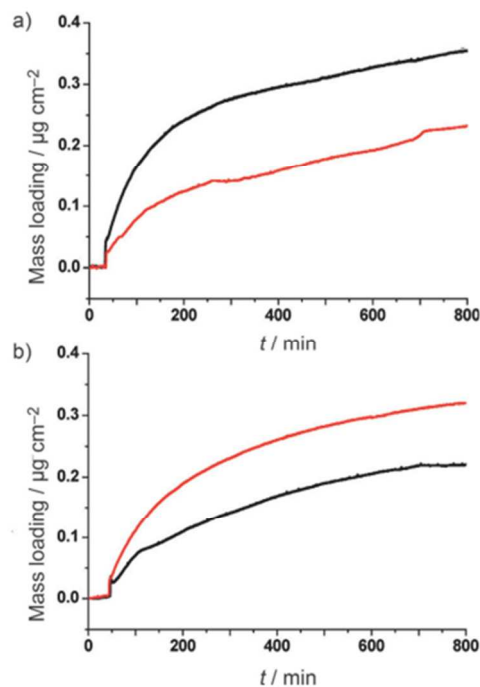


**Fig. 28** QCM profiles for the specific mass uptake of each enantiomer from the gas phase: a) R-HDO (black) and S-HDO (red) over (+)-1 (20 cycles) and b) R-HDO (black) and S-HDO (red) over (-)-1 (20 cycles). The difference in the absolute adsorption values for the two samples may have arisen from a slight difference in the total amount of SURMOF deposited on the QCM substrate surface (Adapted with permission from ref.<sup>157</sup>).

However, only continuously grown and porous substrate-supported membranes can be used in a membrane separation process. As Jin *et al.* reported in 2012, a new generation of chiral separation membrane composed of homochiral Zn-BLD was successfully fabricated on a porous zinc oxide substrate by a reactive seeding technique for the first time.<sup>160</sup> This membrane was stable enough for the chiral separation driven by the concentration difference across the membrane. The resolution process was carried out by a 'side-by-side diffusion cell' and readily separated by the as-prepared membrane, as shown in Fig. 29 (Top). Two chambers connected with a clamp served as the dialyzers and the membrane was placed between them while fluororubber gaskets were used to seal the connection.

The feed and permeate sides were continuously stirred by a magnetic stirring apparatus. The racemic MPS that dissolved in the n-hexane solvent was introduced to the feed side and the pure n-hexane solvent was used at the permeate side. During the permeation experiment, the variations in the MPD concentration at the feed side did not exceed 2%. The concentrations of both enantiomers increased with the permeation time. The R-MPS enantiomer had a higher yield than that of the S-MPS enantiomer. The differences between the concentrations of the two enantiomers became noticeable after permeation for about 18 h. After 48 h of separation, the enantioselectivity appeared to be at its highest and the *ee*<sup>0</sup> reached 33.0%. The preferential diffusion of R-MPS in the Zn-BLD membrane suggested that R-MPS had a weaker affinity for the membrane than S-MPS. This was confirmed by the adsorption separation behaviour of racemic MPSs in the Zn-BLD crystals. The result was further confirmed by the

following simulation data. R-MPS transported faster than S-MPS and the two enantiomers could be separated, in accordance with the experimental data (Fig. 29 Bottom).

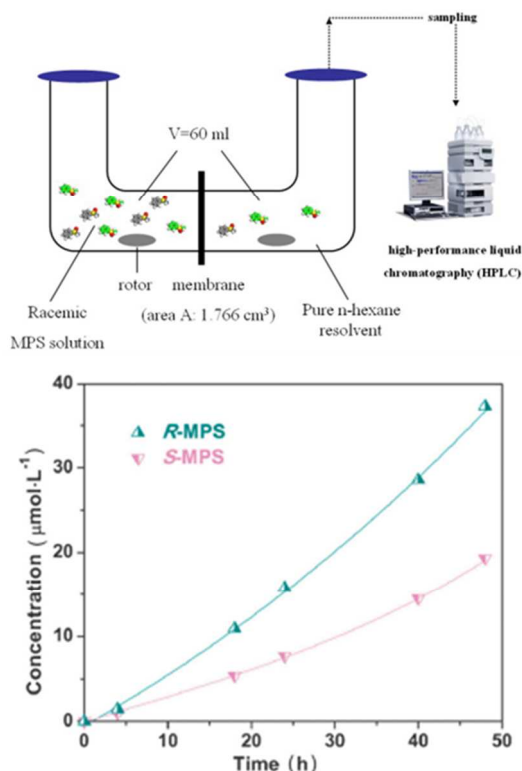


**Fig. 29** Top: Schematic diagram of the side-by-side diffusion cell used for the measurement of the Zn-LBD membrane's chiral separation performance at 25°C. Bottom: R-/S-MPS concentrations on the permeate side of the Zn-BLD membrane as a function of separation time. Initial concentration of racemic MPSs on the donor side was 5 mmolL<sup>-1</sup> (Adapted with permission from ref.<sup>160</sup>).

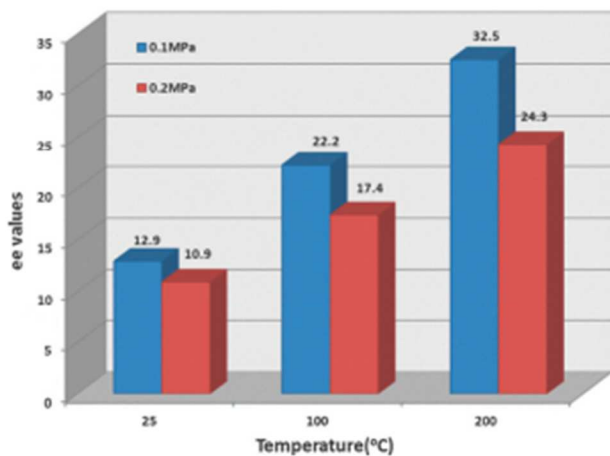


**Fig. 30** Comparison of the *ee* values for racemic diol mixtures at different temperatures and pressures (Adapted with permission from ref.<sup>46</sup>).

In 2013, we reported a chiral MOF Ni<sub>2</sub>(L-asp)<sub>2</sub>(bipy) with neutral chiral Ni(L-asp) layers connected by 4,4'-bipyridine (bipy) linkers to afford a pillared structure.<sup>46</sup> It had a 1D corrugated channel (about 3.8 × 4.7 Å) lined with the chiral carbon atoms of L-aspartic acid (L-asp) ligands.<sup>168</sup> This homochiral MOF possessed the following advantages: (i) it was thermally stable in air, which is very important for separation applications as the structure can be retained up to 300°C; and (ii) L-asp is a low cost, commercially available raw material that can be obtained by catalysed enzymatic reaction. A diol isomer mixture (2-methyl-2,4-pentanediol) was used to test their separation efficiency. The higher penetration amount of R diols through the membrane was largely attributed to our assumption that there was a geometry-dependent interaction between the chiral channel and the optical isomer guests, making it easier for R-diols than for S-diols to enter into the membrane pores. The temperature-pressure-related membrane performance of homochiral MOF membranes was observed for the first time (Fig. 30), and could prove an important issue in the development of chiral resolution. As the temperature increased, fewer S enantiomers were adsorbed and R enantiomers could diffuse in the resulting free volume. Thus, the selectivity of the membrane improved as the temperature increased. The resulting *ee* value reached 32.5% at 200°C. The same MOFs framework was made into a membrane by Jin *et al.* using the secondary growth method.<sup>156</sup> Chiral resolution was conducted using the concentration difference across the membrane. At 30°C, an enantiomeric excess value of 35.5% was obtained at a feed concentration of 1.0 mmolL<sup>-1</sup>.

### 3.2.2 Others

There are some other liquid mixture separations that have been reported using stable MOFs. The related selectivity can be found in Table 4. In addition to the H<sub>2</sub> separation, a MIL-53(Al) membrane was applied to the dehydration of the azeotrope of an ethylacetate (EAC) aqueous solution by pervaporation,<sup>66</sup> as the channel size of the MIL-53 material (7.3×7.7 Å) was larger than the kinetic diameters of most of the small gas molecules. On passing the water–EAC mixtures (7 wt% water) through the MIL-53 membrane, the permeate water concentration increased to 99wt% with an accompanying flux of 454 gm<sup>-2</sup>h<sup>-1</sup> at 60°C. The high selectivity of the MIL-53 membrane was attributed largely to our assumption that many hydroxyl groups existed on the MIL-53 membrane's surface, and that they could form hydrogen bonds with the H<sub>2</sub>O. Thus, it was easier for H<sub>2</sub>O to enter the membrane pores than it was for EAC molecules. The hydrothermal stability of the membranes was tested by using the MIL-53 membrane in a pervaporation process for a long period. The prepared membrane exhibited very good stability after more than 200 h of operation.

Supported polycrystalline ZIF-8 membranes were evaluated by separating the liquid mixtures of n-hexane/benzene and n-hexane/mesitylene as feeds in pervaporation experiments at room temperature.<sup>158</sup> Even considering the framework flexibility that has already proven to spoil a clear cut off in the separation performance of ZIF-8 in light gas permeation experiments, bulky aromatic compounds should not be able to enter the framework, and a molecular sieve exclusion separation was expected. Surprisingly, this sharp separation could not be found experimentally. Accordingly, simple liquid adsorption experiments were conducted with mixtures of the hydrocarbons under study and ethanol. The measurements

qualitatively showed that n-hexane and benzene were adsorbed by ZIF-8, but mesitylene was not. This corresponded to the trend found in pervaporation experiments, in which the real mixture separation factor is lower than the predicted ideal permselectivity for n-hexane/benzene compared to n-hexane/mesitylene, because the more mobile component (n-hexane) is blocked by the less mobile component (benzene). In contrast, for n-hexane/mesitylene, molecular sieving occurs with increasing mesitylene concentration in the binary mixture. The flux of n-hexane is thus increasingly reduced by pore entrance blocking. This finding is in complete accordance with the model in which a non-transporting bulky molecule blocks the pore entrances for the mobile component, as observed in the sorption kinetics of n-decane on 5A zeolites from nonadsorbing solvents.

Lin *et al.* reported a ZIF-71 membrane prepared on a porous ZnO substrate by a reactive seeding method, and he used it in the pervaporation separation of liquid alcohol–water and dimethyl carbonate–methanol mixtures.<sup>159</sup> Before the pervaporation analysis, the contact angles of water, methanol and ethanol on the ZIF-71 membranes were measured. The static contact angle of water on the membrane was about 92.11, indicating that the surface of the ZIF-71 membrane was not highly hydrophobic. The static contact angles of methanol and ethanol on the membranes could not be observed because they could get into the pores of the ZIF-71 immediately. Therefore, only the dynamic decrease processes of the contact angles could be seen, indicating that both the outer and inner surfaces of ZIF-71 were organophilic, making it a promising membrane material for the pervaporation separation of organic molecules. The permeation process was governed by both adsorption and diffusion. Although the strong organophilic properties of ZIF-71 provided favourable adsorption of ethanol molecules onto the ZIF-71 membrane, the diffusion of ethanol was relatively slow because the ethanol kinetic diameter (4.53 Å) was close to the window size of ZIF-71 (nominal 4.8 Å). In contrast, the diffusion of methanol (with a kinetic diameter of 3.63 Å) in the ZIF-71 channel was relatively fast, resulting in better separation performance. DMC/MeOH separation was also conducted on this membrane, and it exhibited a good DMC permselectivity of 5.34. Although the kinetic diameter of the methanol was smaller than that of the DMC (4.7 Å < DMC < 6.3 Å), the DMC preferentially permeated through the membrane due to the difference in the polarity between methanol and DMC. In addition, the DMC was larger than the window size of the ZIF-71 membrane, yet the former could diffuse through the latter. This is a widely observed phenomenon in ZIF membranes, as is the removal of DMF molecules from the ZIF crystal with a relatively small pore size.

In recent work, a MOF membrane was applied in the separation of cyclohexanone and cyclohexanol – important organic intermediates in the petrochemical industry that are difficult to separate – for the first time.<sup>161</sup> The MOF structure selected for membrane synthesis in this work was ZIF-78, due to its appropriate pore size, considerable nitro groups in the framework and relative stability. In the initial stage (0–16 h), there was a distinct decrease in the total permeation flux, which swung slightly above and below a certain value in the remaining time, maintaining stable throughout. The average total permeation flux ( $9.3 \times 10^{-2} \text{ kgm}^{-2}\text{h}^{-1}$ ) is finally achieved. Similar to the situation of flux, the separation factor also showed a downward trend at the beginning. It kept reducing from about 4.0–0.5 until equilibrium was established. During equilibrium, the molecules of cyclohexanol diffused stably

twice as fast as the cyclohexanone molecules in the permeation. The prepared ZIF-78 membrane was not pre-exchanged by other solvents after synthesis to avoid any negative effect on the structure. The slow exchanging process of guests began when we started circulating the mixture solution on the feed side of the membrane and evacuating on the permeate side. DMF molecules confined in the pores gradually diffused outwards from the crystal layer to the permeate side under vacuum and the vacancies left were filled with cyclohexanone and cyclohexanol. Due to the slight difference in spatial configuration, it was slightly easier for cyclohexanone to enter the framework than for cyclohexanol to do so. Furthermore, most of the cyclohexanol molecules that had gone into the pores interacted with the nitro groups from the framework by forming hydrogen bonds. Thus, there were more cyclohexanone molecules permeating through the membrane at first. As the testing process continued, more cyclohexanol molecules gathered inside the pores, increasing resistance for molecules to pass by. Therefore, the number of permeating cyclohexanol molecules gradually increased until the equilibrium was established. There were two main reasons for the decline of the total flux in the earlier stage. First, the molecules of cyclohexanone and cyclohexanol encountered greater steric hindrance in the pores than did the guest DMF. Second, when the cyclohexanol molecules entered the ZIF-78 framework, the stronger binding force with the -NO<sub>2</sub> groups not only further reduced their diffusion rate, but also hindered the movement of cyclohexanone molecules.

### 3.3 Stability of MOF membranes

The durability and repeatability of membrane materials are very important elements in achieving industrial separation application. To address this issue, researchers must select stable structures that are also easy to synthesise. Several classic MOF materials with separation properties have been made into membranes, such as the MOF-5, HKUST-1, MIL-53 and ZIFs, etc. However, flexibility and instability are critical issues which limit the application of MOF membranes. One of the major drawbacks is their poor hydrothermal stability, which is clearly a limitation to their practical applications. For example, MOF-5 can readily change phase to a nonporous structure in ambient humidity.

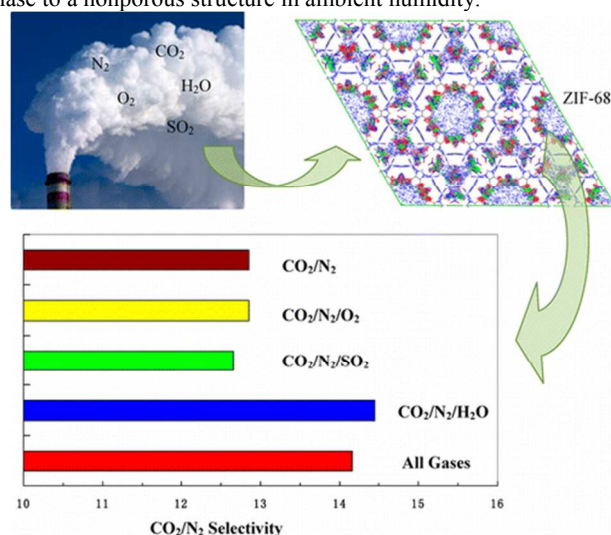


**Fig. 31** Scheme of effects of water vapor and other gas impurities in flue gas on CO<sub>2</sub>/N<sub>2</sub> separation using ZIF-68 (Adapted with permission from ref.<sup>169</sup>).

Very recently, ZIF-8 membranes in solvents especially water has been found.<sup>71, 101, 103</sup> In 2014, Lin *et al.* successfully prepared thin (2.5  $\mu\text{m}$ ), high quality ZIF-8 membranes in aqueous solutions and focused on understanding permeation and separation properties of propylene/propane mixture of the ZIF-8 membranes. This work has shown that ZIF-8 membranes are extremely stable under both off-stream storage and on-stream propylene/propane separation conditions. The excellent stability, as well as the good separation performances, makes ZIF-8 membrane very attractive for propylene/propane separation in industrial applications.

In realistic separation systems, mixtures and conditions are very complicated. Recently, Liu *et al.* simulated the effects of the presence of water vapor and other gas impurities (such as  $\text{SO}_2$  and  $\text{O}_2$ ) in flue gas on the performance of  $\text{CO}_2$  adsorption on the ZIF-68 material (Fig. 31).<sup>169</sup> The results showed that the presence of  $\text{O}_2$  has a negligible effect on  $\text{CO}_2$  adsorption on ZIF-68.  $\text{H}_2\text{O}$  affects the  $\text{CO}_2$  adsorption on ZIF-68 in two opposite ways: reduces the  $\text{CO}_2$  adsorption ability due to the negative effect, but increases the  $\text{CO}_2/\text{N}_2$  separation factor due to the positive effect. However, the presence of  $\text{SO}_2$  inhibits both the  $\text{CO}_2$  adsorption and the  $\text{CO}_2/\text{N}_2$  separation abilities of ZIF-68. Of course the results of the simulation should be compared with experimental results.

So development of MOF membranes with high stability is an important research topic for practical separation applications. In addition, there are still some super stable MOFs based on zirconium clusters,<sup>170-174</sup> that have not yet been made into membranes due to the intergrowth problem probably.

#### 4. Conclusions and Outlook

As described in the recent review written by Yaghi *et al.* in *Science*,<sup>104</sup> more than 20,000 different MOFs have been reported and studied within the past decade – a number that is continuously growing. The surface area values of such MOFs typically range from 1000 to 10,000  $\text{m}^2/\text{g}$ , exceeding those of traditional porous materials such as zeolites and carbons. In addition to the surface area, MOFs with permanent porosity are more extensive in their variety and multiplicity than any other class of porous materials due to their wonderful designability and flexibility. All these aspects have made MOFs ideal candidate materials for membranes in separation processes. As with the development of zeolite membranes, both the preparation and application of MOF membranes are undergoing tremendous progress. Following the pioneering work using a complex method to fabricate membranes on limited supports, the methods and substrates have been expanded like a hundred flowers in bloom. For instance, as we discussed in Section 2, some scale-up or convenient processing technologies (e.g. electrospinning and ‘twin copper source’) have been developed for the preparation of crack-free MOF membranes. Simultaneously, efforts have also been made to upgrade the efficacies of some important separations. As  $\text{H}_2$  purification is closely related to energy and the environment, the performance of the membrane for separating  $\text{H}_2$  from other gases has been significantly improved through post-functionalisation processes or molecular sieving using a suitable structure. Recently, the separation range of MOF membranes has not been limited to the simple separation of gas molecules. Many vital and useful separation issues have been solved by this type of material via the advantage of structural diversities.

There is still a long way to go in achieving the practical application of MOF membranes in separation processes. For the

synthesis system, some reaction mechanisms and condition choices still require detailed study. More importantly, simple, low-cost methods are being developed to prepare more types of large-scale MOFs on economical supports. Regarding application, we believe this is just the beginning for MOF membranes. Their stability and cracking problems may be solved by doping them with other species to form mixed-matrix membranes (MMMs).<sup>105, 175</sup> Depending on the variety of structures and function groups, an increasing number of mixture separations will be studied using MOF membranes and some systematically varied and smart gating membranes will be developed for effective separation. Likewise, special ultra-large-pore MOF membranes may prove promising in biological molecule separations.

#### Acknowledgements

This work was supported by National Natural Science Foundation of China (21390394), the National Basic Research Program of China (2012CB821700, 2011CB808703), NSFC (21101072, 21261130584, 91022030), “111” project (B07016), and Award Project of KAUST (CRG-1-2012-LAI-009).

#### Primary Sources

#### Secondary Sources

#### Uncategorized References

1. M. Eddaoudi, D. B. Moler, H. Li, B. Chen, T. M. Reineke, M. O’Keeffe and O. M. Yaghi, *Accounts of Chemical Research*, 2001, **34**, 319-330.
2. J. R. Li, R. J. Kuppler and H. C. Zhou, *Chemical Society reviews*, 2009, **38**, 1477-1504.
3. J.-R. Li, J. Sculley and H.-C. Zhou, *Chemical reviews*, 2012, **112**, 869-932.
4. P. Nugent, Y. Belmabkhout, S. D. Burd, A. J. Cairns, R. Luebke, K. Forrest, T. Pham, S. Ma, B. Space, L. Wojtas, M. Eddaoudi and M. J. Zaworotko, *Nature*, 2013, **495**, 80-84.
5. Y. Sakata, S. Furukawa, M. Kondo, K. Hirai, N. Horike, Y. Takashima, H. Uehara, N. Louvain, M. Meilikhov, T. Tsuruoka, S. Isoda, W. Kosaka, O. Sakata and S. Kitagawa, *Science*, 2013, **339**, 193-196.
6. P. Tung Cao Thanh, H. S. Kim and K. B. Yoon, *Science*, 2011, **334**, 1533-1538.
7. Q. Ge, Z. Wang and Y. Yan, *J. Am. Chem. Soc.*, 2009, **131**, 17056-17057.
8. B. Chen, S. Xiang and G. Qian, *Acc. Chem. Res.*, 2010, **43**, 1115-1124.
9. R. W. Baker, *Ind. Eng. Chem. Res.*, 2002, **41**, 1393-1411.
10. Z. P. Lai, G. Bonilla, I. Diaz, J. G. Nery, K. Sujaoti, M. A. Amat, E. Kokkoli, O. Terasaki, R. W. Thompson, M. Tsapatsis and D. G. Vlachos, *Science*, 2003, **300**, 456-460.
11. X. Yin, G. Zhu, W. Yang, Y. Li, G. Zhu, R. Xu, J. Sun, S. Qiu and R. Xu, *Advanced materials*, 2005, **17**, 2006-2010.
12. H. Guo, G. Zhu, H. Li, X. Zou, X. Yin, W. Yang, S. Qiu and R. Xu, *Angewandte Chemie-International Edition*, 2006, **45**, 7053-7056.
13. J. Caro and M. Noack, *Microporous and Mesoporous Materials*, 2008, **115**, 215-233.
14. M. Yu, R. D. Noble and J. L. Falconer, *Accounts of Chemical Research*, 2011, **44**, 1196-1206.
15. Y. S. Lin, I. Kumakiri, B. N. Nair and H. Alsayouri, *Sep. Purif. Methods*, 2002, **31**, 229-369.
16. J. Choi, H.-K. Jeong, M. A. Snyder, J. A. Stoeger, R. I. Masel and M. Tsapatsis, *Science*, 2009, **325**, 590-593.
17. M. Shah, M. C. McCarthy, S. Sachdeva, A. K. Lee and H.-K. Jeong, *Industrial & Engineering Chemistry Research*, 2012, **51**, 2179-2199.

18. J. Coronas and J. Santamaría, *Separation & Purification Reviews*, 1999, **28**, 127-177.
19. J. Gascon and F. Kapteijn, *Angewandte Chemie*, 2010, **49**, 1530-1532.
20. S. Qiu and G. Zhu, *Coordination Chemistry Reviews*, 2009, **253**, 2891-2911.
21. G. R. Gavalas, *Zeolite membranes for gas and liquid separations* John Wiley & Sons Ltd., West Sussex, 2006.
22. X. Zou, G. Zhu, F. Zhang, M. Guo and S. Qiu, *CrystEngComm*, 2010, **12**, 352.
23. J. Liu, F. Zhang, X. Zou, S. Zhou, L. Li, F. Sun and S. Qiu, *European Journal of Inorganic Chemistry*, 2012, **2012**, 0-0.
24. S. Hermes, F. Schroder, R. Chelmoski, C. Woll and R. A. Fischer, *Journal of the American Chemical Society*, 2005, **127**, 13744-13745.
25. M. Arnold, P. Kortunov, D. J. Jones, Y. Nedellec, J. Kaerger and J. Caro, *European Journal of Inorganic Chemistry*, 2007, 60-64.
26. E. Biemmi, C. Scherb and T. Bein, *J. Am. Chem. Soc.*, 2007, **129**, 8054-8055.
27. C. Scherb, A. Schodel and T. Bein, *Angew. Chem., Int. Ed.*, 2008, **47**, 5777-5779.
28. J. Gascon, S. Aguado and F. Kapteijn, *Microporous Mesoporous Mater.*, 2008, **113**, 132-138.
29. X. Zou, G. Zhu, I. J. Hewitt, F. Sun and S. Qiu, *Dalton transactions*, 2009, 3009-3013.
30. J. Liu, F. Sun, F. Zhang, Z. Wang, R. Zhang, C. Wang and S. Qiu, *Journal of Materials Chemistry*, 2011, **21**, 3775.
31. J. Caro, *Current Opinion in Chemical Engineering*, 2011, **1**, 77-83.
32. J. Gascon, F. Kapteijn, B. Zornoza, V. Sebastián, C. Casado and J. Coronas, *Chemistry of Materials*, 2012, **24**, 2829-2844.
33. Y. Liu, Z. Ng, E. A. Khan, H.-K. Jeong, C.-b. Ching and Z. Lai, *Microporous and Mesoporous Materials*, 2009, **118**, 296-301.
34. R. Ranjan and M. Tsapatsis, *Chemistry of Materials*, 2009, **21**, 4920-4924.
35. H. Bux, F. Liang, Y. Li, J. Cravillon, M. Wiebcke and J. Caro, *Journal of the American Chemical Society*, 2009, **131**, 16000-16001.
36. N. Stock and S. Biswas, *Chemical reviews*, 2012, **112**, 933-969.
37. D. Zacher, O. Shekhah, C. Woll and R. A. Fischer, *Chemical Society reviews*, 2009, **38**, 1418-1429.
38. B. Liu and R. A. Fischer, *Science China Chemistry*, 2011, **54**, 1851-1866.
39. O. Shekhah, J. Liu, R. A. Fischer and C. Woll, *Chemical Society reviews*, 2011, **40**, 1081-1106.
40. D. Zacher, R. Schmid, C. Woll and R. A. Fischer, *Angewandte Chemie*, 2011, **50**, 176-199.
41. A. Betard and R. A. Fischer, *Chemical reviews*, 2012, **112**, 1055-1083.
42. D. Bradshaw, A. Garai and J. Huo, *Chemical Society reviews*, 2012, **41**, 2344-2381.
43. S. Bertazzo and K. Rezwan, *Langmuir : the ACS journal of surfaces and colloids*, 2009, **26**, 3364-3371.
44. Y. Liu, E. Hu, E. A. Khan and Z. Lai, *Journal of Membrane Science*, 2010, **353**, 36-40.
45. H. Guo, G. Zhu, I. J. Hewitt and S. Qiu, *Journal of the American Chemical Society*, 2009, **131**, 1646-1647.
46. Z. Kang, M. Xue, L. Fan, J. Ding, L. Guo, L. Gao and S. Qiu, *Chemical communications*, 2013, **49**, 10569-10571.
47. F. Schreiber, *Prog. Surf. Sci.*, 2000, **65**, 151-256.
48. J. C. Love, L. A. Estroff, J. K. Kriebel, R. G. Nuzzo and G. M. Whitesides, *Chem. Rev.*, 2005, **105**, 1103-1169.
49. M. Kind and C. Wöll, *Prog. Surf. Sci.*, 2009, **84**, 230-278.
50. B. C. Bunker, P. C. Rieke, B. J. Tarasevich, A. A. Campbell, G. E. Fryxell, G. L. Graff, L. Song, J. Liu, J. W. Virden and G. L. McVay, *Science*, 1994, **264**, 48-55.
51. S. Feng and T. Bein, *Nature*, 1994, **368**, 834-836.
52. J. Aizenberg, A. J. Black and G. M. Whitesides, *J. Am. Chem. Soc.*, 1999, **121**, 4500-4509.
53. F. C. Meldrum, J. Flath and W. Knoll, *J. Mater. Chem.*, 1999, **9**, 711-723.
54. J. W. P. Hsu, Z. R. Tian, N. C. Simmons, C. M. Matzke, J. A. Voigt and J. Liu, *Nano Lett.*, 2005, **5**, 83-86.
55. J. S. Lee, Y.-J. Lee, E. L. Tae, Y. S. Park and K. B. Yoon, *Science*, 2003, **301**, 818-821.
56. D. Wang, J. Liu, Q. Huo, Z. Nie, W. Lu, R. E. Williford and Y.-B. Jiang, *J. Am. Chem. Soc.*, 2006, **128**, 13670-13671.
57. A. Huang, W. Dou and J. Caro, *Journal of the American Chemical Society*, 2010, **132**, 15562-15564.
58. A. Huang, H. Bux, F. Steinbach and J. Caro, *Angewandte Chemie*, 2010, **49**, 4958-4961.
59. M. C. McCarthy, V. V. Guerrero, G. V. Barnett and H.-K. Jeong, *Langmuir : the ACS journal of surfaces and colloids*, 2010, **26**, 14636-14641.
60. T. Ben, C. Lu, C. Pei, S. Xu and S. Qiu, *Chemistry*, 2012, **18**, 10250-10253.
61. H. T. Kwon and H. K. Jeong, *Journal of the American Chemical Society*, 2013, **135**, 10763-10768.
62. H. Guo, Y. Zhu, S. Qiu, J. A. Lercher and H. Zhang, *Advanced materials*, 2010, **22**, 4190-4192.
63. F. Zhang, X. Zou, X. Gao, S. Fan, F. Sun, H. Ren and G. Zhu, *Advanced Functional Materials*, 2012, **22**, 3583-3590.
64. L. Fan, M. Xue, Z. Kang, H. Li and S. Qiu, *Journal of Materials Chemistry*, 2012, **22**, 25272-25276.
65. L. Fan, M. Xue, Z. Kang and S. Qiu, *Science China Chemistry*, 2013, **56**, 459-464.
66. Y. Hu, X. Dong, J. Nan, W. Jin, X. Ren, N. Xu and Y. M. Lee, *Chemical communications*, 2011, **47**, 737-739.
67. O. Shekhah, H. Wang, S. Kowarik, F. Schreiber, M. Paulus, M. Tolan, C. Sternemann, F. Evers, D. Zacher, R. A. Fischer and C. Wöll, *Journal of the American Chemical Society*, 2007, **129**, 15118 - 15119.
68. R. Makiura, S. Motoyama, Y. Umemura, H. Yamanaka, O. S. O and H. Kitagawa, *Nat. Mater.*, 2010, **9**, 565-571.
69. J. Nan, X. Dong, W. Wang, W. Jin and N. Xu, *Langmuir : the ACS journal of surfaces and colloids*, 2011, **27**, 4309-4312.
70. A. Huang and J. Caro, *Angewandte Chemie*, 2011, **50**, 4979-4982.
71. X. Liu, Y. Li, Y. Ban, Y. Peng, H. Jin, H. Bux, L. Xu, J. Caro and W. Yang, *Chemical communications*, 2013, **49**, 9140-9142.
72. S. Takamizawa, Y. Takasaki and R. Miyake, *Journal of the American Chemical Society*, 2010, **132**, 2862-2863.
73. Y. S. Li, F. Y. Liang, H. Bux, A. Feldhoff, W. S. Yang and J. Caro, *Angewandte Chemie*, 2010, **49**, 548-551.
74. Y. Li, F. Liang, H. Bux, W. Yang and J. Caro, *Journal of Membrane Science*, 2010, **354**, 48-54.
75. Y. S. Li, H. Bux, A. Feldhoff, G. L. Li, W. S. Yang and J. Caro, *Advanced materials*, 2010, **22**, 3322-3326.
76. J. Yao, D. Dong, D. Li, L. He, G. Xu and H. Wang, *Chemical communications*, 2011, **47**, 2559-2561.
77. H. Bux, A. Feldhoff, J. Cravillon, M. Wiebcke, Y.-S. Li and J. Caro, *Chemistry of Materials*, 2011, **23**, 2262-2269.
78. K. Huang, S. Liu, Q. Li and W. Jin, *Separation and Purification Technology*, 2013, **119**, 94-101.
79. A. Huang, Y. Chen, N. Wang, Z. Hu, J. Jiang and J. Caro, *Chemical communications*, 2012, **48**, 10981-10983.
80. X. Dong, K. Huang, S. Liu, R. Ren, W. Jin and Y. S. Lin, *Journal of Materials Chemistry*, 2012, **22**, 19222-19227.
81. S. Zhou, X. Zou, F. Sun, H. Ren, J. Liu, F. Zhang, N. Zhao and G. Zhu, *International Journal of Hydrogen Energy*, 2013, **38**, 5338-5347.
82. A. Huang, Y. Chen, Q. Liu, N. Wang, J. Jiang and J. Caro, *Journal of Membrane Science*, 2014, **454**, 126-132.
83. Y. Yoo, Z. Lai and H.-K. Jeong, *Microporous and Mesoporous Materials*, 2009, **123**, 100-106.
84. Z. Zhao, X. Ma, Z. Li and Y. S. Lin, *Journal of Membrane Science*, 2011, **382**, 82-90.
85. D. Nagaraju, D. G. Bhagat, R. Banerjee and U. K. Kharul, *Journal of Materials Chemistry A*, 2013, **1**, 8828.
86. S. Zhou, X. Zou, F. Sun, F. Zhang, S. Fan, H. Zhao, T. Schiestel and G. Zhu, *Journal of Materials Chemistry*, 2012, **22**, 10322.
87. S. Fan, F. Sun, J. Xie, J. Guo, L. Zhang, C. Wang, Q. Pan and G. Zhu, *Journal of Materials Chemistry A*, 2013, **1**, 11438.
88. D.-J. Lee, Q. Li, H. Kim and K. Lee, *Microporous and Mesoporous Materials*, 2012, **163**, 169-177.

89. Z. Xie, T. Li, N. L. Rosi and M. A. Carreon, *Journal of Materials Chemistry A*, 2014, **2**, 1239.
90. S. R. Venna and M. A. Carreon, *Journal of the American Chemical Society*, 2009, **132**, 76–78.
91. A. Bétard, H. Bux, S. Henke, D. Zacher, J. Caro and R. A. Fischer, *Microporous and Mesoporous Materials*, 2012, **150**, 76–82.
92. X. Zou, F. Zhang, S. Thomas, G. Zhu, V. Valtchev and S. Mintova, *Chem. Eur. J.*, 2011, **17**, 12076–12083.
93. Y. Liu, G. Zeng, Y. Pan and Z. Lai, *Journal of Membrane Science*, 2011, **379**, 46–51.
94. S. Aguado, C.-H. Nicolas, V. Moizan-Baslé, C. Nieto, H. Amrouche, N. Bats, N. Audebrand and D. Farrusseng, *New Journal of Chemistry*, 2011, **35**, 41–44.
95. Y. Yoo, V. Varela-Guerrero and H. K. Jeong, *Langmuir: the ACS journal of surfaces and colloids*, 2011, **27**, 2652–2657.
96. J. A. Bohrman and M. A. Carreon, *Chemical communications*, 2012, **48**, 5130–5132.
97. H. Bux, C. Chmelik, R. Krishna and J. Caro, *Journal of Membrane Science*, 2011, **369**, 284–289.
98. M. N. Shah, M. A. Gonzalez, M. C. McCarthy and H. K. Jeong, *Langmuir: the ACS journal of surfaces and colloids*, 2013, **29**, 7896–7902.
99. H. T. Kwon and H. K. Jeong, *Chemical communications*, 2013, **49**, 3854–3856.
100. N. Hara, M. Yoshimune, H. Negishi, K. Haraya, S. Hara and T. Yamaguchi, *Journal of Membrane Science*, 2014, **450**, 215–223.
101. D. Liu, X. Ma, H. Xi and Y. S. Lin, *Journal of Membrane Science*, 2014, **451**, 85–93.
102. Y. Pan, T. Li, G. Lestari and Z. Lai, *Journal of Membrane Science*, 2012, **390–391**, 93–98.
103. Y. Pan and Z. Lai, *Chemical communications*, 2011, **47**, 10275–10277.
104. H. Furukawa, K. E. Cordova, M. O’Keeffe and O. M. Yaghi, *Science*, 2013, **341**, 1230444.
105. I. Erucar, G. Yilmaz and S. Keskin, *Chemistry, an Asian journal*, 2013, **8**, 1692–1704.
106. M. Anderson, H. Wang and Y. S. Lin, *Reviews in Chemical Engineering*, 2012, **28**, 101–121.
107. C. C. H. Lin, K. A. Dambrowitz and S. M. Kuznicki, *Canadian Journal of Chemical Engineering*, 2012, **90**, 207–216.
108. M. Yu, R. D. Noble and J. L. Falconer, *Accounts of Chemical Research*, 2011, **44**, 1196–1206.
109. Y. S. Lin, I. Kumakiri, B. N. Nair and H. Alsayouri, *Separation and Purification Methods*, 2002, **31**, 229–379.
110. J. Gascon, F. Kapteijn, B. Zornoza, V. Sebastian, C. Casado and J. Coronas, *Chemistry of Materials*, 2012, **24**, 2829–2844.
111. T. Hijikata, *International Journal of Hydrogen Energy*, 2002, **27**, 115–129.
112. B. Freeman, Y. Yampolskii and I. Pinnau, *Materials science of membranes for gas and vapor separation. 1st ed.*, Wiley, 2006.
113. S. S. Y. Chui, S. M. F. Lo, J. P. H. Charmant, A. G. Orpen and I. D. Williams, *Science*, 1999, **283**, 1148–1150.
114. H. Bux, C. Chmelik, J. M. van Baten, R. Krishna and J. Caro, *Advanced materials*, 2010, **22**, 4741–4743.
115. H. Wu, W. Zhou and T. Yildirim, *Journal of the American Chemical Society*, 2007, **129**, 5314–5315.
116. H. Wu, W. Zhou and T. Yildirim, *Journal of Physical Chemistry C*, 2009, **113**, 3029–3035.
117. W. Zhou, H. Wu, M. R. Hartman and T. Yildirim, *Journal of Physical Chemistry C*, 2007, **111**, 16131–16137.
118. K. S. Park, Z. Ni, A. P. Cote, J. Y. Choi, R. Huang, F. J. Uribe-Romo, H. K. Chae, M. O’Keeffe and O. M. Yaghi, *Proceedings of the National Academy of Sciences of the United States of America*, 2006, **103**, 10186–10191.
119. X. C. Huang, J. P. Zhang and X. M. Chen, *Chinese Science Bulletin*, 2003, **48**, 1531–1534.
120. X. C. Huang, Y. Y. Lin, J. P. Zhang and X. M. Chen, *Angewandte Chemie-International Edition*, 2006, **45**, 1557–1559.
121. M. Hong, J. L. Falconer and R. D. Noble, *Industrial & Engineering Chemistry Research*, 2005, **44**, 4035–4041.
122. M. Kanezashi, J. O’Brien-Abraham, Y. S. Lin and K. Suzuki, *Aiche Journal*, 2008, **54**, 1478–1486.
123. H. Hayashi, A. P. Côté, H. Furukawa, M. O’Keeffe and O. M. Yaghi, *Nat. Mater.*, 2007, **6**, 501–506.
124. W. Morris, C. J. Doonan, H. Furukawa, R. Banerjee and O. M. Yaghi, *Journal of the American Chemical Society*, 2008, **130**, 12626–12627.
125. J. R. Rostrup-Nielsen and T. Rostrup-Nielsen, *Cattech*, 2002, **6**, 150–159.
126. A. D. Burrows, C. G. Frost, M. F. Mahon and C. Richardson, *Angewandte Chemie-International Edition*, 2008, **47**, 8482–8486.
127. T. Haneda, M. Kawano, T. Kawamichi and M. Fujita, *Journal of the American Chemical Society*, 2008, **130**, 1578–1579.
128. Z. Wang and S. M. Cohen, *Angewandte Chemie-International Edition*, 2008, **47**, 4699–4702.
129. T. Loiseau, C. Serre, C. Huguenard, G. Fink, F. Taulelle, M. Henry, T. Bataille and G. Férey, *Chem.–Eur. J.*, 2004, **10**, 1373–1382.
130. S. Couck, J. F. M. Denayer, G. V. Baron, T. Remy, J. Gascon and F. Kapteijn, *J. Am. Chem. Soc.*, 2009, **131**, 6326–6327.
131. T. Okubo and H. Inoue, *AIChE J.*, 1989, **35**, 845–848.
132. B. Wang, A. P. Cote, H. Furukawa, M. O’Keeffe and O. M. Yaghi, *Nature*, 2008, **453**, 207–211.
133. K. Uemura, A. Maeda, T. K. Maji, P. Kanoo and H. Kita, *European Journal of Inorganic Chemistry*, 2009, **2009**, 2329–2337.
134. S. Noro, S. Kitagawa, M. Kondo and K. Seki, *Angew. Chem. Int. Ed.*, 2000, **39**, 2082–2084.
135. H. Knight, *New Scientist*, 2010, **206**, 44–47.
136. Y. F. Makogon, *Journal of Natural Gas Science and Engineering*, 2010, **2**, 49–59.
137. R. F. Service, *Science*, 2004, **305**, 962–963.
138. H. Q. Lin, E. Van Wagner, R. Raharjo, B. D. Freeman and I. Roman, *Advanced materials*, 2006, **18**, 39–44.
139. W. Xu, P. Blazkiewicz and S. Fleming, *Advanced materials*, 2001, **13**, 1014–1018.
140. L. Liu, A. Chakma and X. S. Feng, *Industrial & Engineering Chemistry Research*, 2005, **44**, 6874–6882.
141. K. Weh, M. Noack, I. Sieber and J. Caro, *Microporous and Mesoporous Materials*, 2002, **54**, 27–36.
142. T. Tomita, K. Nakayama and H. Sakai, *Microporous and Mesoporous Materials*, 2004, **68**, 71–75.
143. J. van den Bergh, W. Zhu, J. Gascon, J. A. Moulijn and F. Kapteijn, *Journal of Membrane Science*, 2008, **316**, 35–45.
144. Y. Cui, H. Kita and K. Okamoto, *Journal of Materials Chemistry*, 2004, **14**, 924–932.
145. M. A. Carreon, S. Li, J. L. Falconer and R. D. Noble, *Journal of the American Chemical Society*, 2008, **130**, 5412–+.
146. J. Lindmark and J. Hedlund, *Journal of Materials Chemistry*, 2010, **20**, 2219–2225.
147. F. Zhang, X. Zou, F. Sun, H. Ren, Y. Jiang and G. Zhu, *CrystEngComm*, 2012, **14**, 5487.
148. R. Banerjee, A. Phan, B. Wang, C. Knobler, H. Furukawa, M. O’Keeffe and O. M. Yaghi, *Science*, 2008, **319**, 939–943.
149. R. L. Burns and W. J. Koros, *Journal of Membrane Science*, 2003, **211**, 299–309.
150. I. G. Giannakopoulos and V. Nikolakis, *Industrial & Engineering Chemistry Research*, 2005, **44**, 226–230.
151. M. L. Chng, Y. Xiao, T.-S. Chung, M. Toriida and S. Tamai, *Carbon*, 2009, **47**, 1857–1866.
152. C. Zhang, Y. Dai, J. R. Johnson, O. Karvan and W. J. Koros, *Journal of Membrane Science*, 2012, **389**, 34–42.
153. M. T. Ravanchi, T. Kaghazchi and A. Kargari, *Desalination*, 2009, **235**, 199–244.
154. M. P. Bernal, J. Coronas, M. Menendez and J. Santamaria, *Journal of Membrane Science*, 2002, **195**, 125–138.
155. K. Li, D. H. Olson, J. Seidel, T. J. Emge, H. Gong, H. Zeng and J. Li, *Journal of the American Chemical Society*, 2009, **131**, 10368–10369.
156. K. Huang, X. Dong, R. Ren and W. Jin, *AIChE Journal*, 2013, **59**, 4364–4372.
157. B. Liu, O. Shekhah, H. K. Arslan, J. Liu, C. Woll and R. A. Fischer, *Angewandte Chemie*, 2012, **51**, 807–810.
158. L. Diestel, H. Bux, D. Wachsmuth and J. Caro, *Microporous and Mesoporous Materials*, 2012, **164**, 288–293.

## Journal Name

159. X. Dong and Y. S. Lin, *Chemical communications*, 2013, **49**, 1196-1198.
160. W. Wang, X. Dong, J. Nan, W. Jin, Z. Hu, Y. Chen and J. Jiang, *Chemical communications*, 2012, **48**, 7022-7024.
161. L. Fan, M. Xue, Z. Kang, G. Wei, L. Huang, J. Shang, D. Zhang and S. Qiu, *Microporous and Mesoporous Materials*, 2013.
162. Z. Kang, J. Ding, L. Fan, M. Xue, D. Zhang, L. Gao and S. Qiu, *Inorganic Chemistry Communications*, 2013, **30**, 74-78.
163. Z. Wang, Q. Ge, J. Shao and Y. Yan, *Journal of the American Chemical Society*, 2009, **131**, 6910-6911.
164. A. N. Collins, G. N. Sheldrake and J. Crosby, *Chirality in Industry*, Wiley, New York, 1992.
165. H. Y. AbouL-enein and I. W. Wainer, *The Impact of Stereochemistry on Drug Development and Use*, Wiley, New York, 1997.
166. X. J. Yin, G. S. Zhu, W. S. Yang, Y. S. Li, G. Q. Zhu, R. Xu, J. Y. Sun, S. L. Qiu and R. R. Xu, *Advanced materials*, 2005, **17**, 2006-+.
167. Y. Liu, M. Sun, C. M. Lew, J. Wang and Y. Yan, *Advanced Functional Materials*, 2008, **18**, 1732-1738.
168. J. P. Barrio, J.-N. Rebilly, B. Carter, D. Bradshaw, J. Bacsá, A. Y. Ganin, H. Park, A. Trewin, R. Vaidhyathan, A. I. Cooper, J. E. Warren and M. J. Rosseinsky, *Chemistry-a European Journal*, 2008, **14**, 4521-4532.
169. Y. Liu, J. Liu, Y. S. Lin and M. Chang, *The Journal of Physical Chemistry C*, 2014, **118**, 6744-6751.
170. J. H. Cavka, S. Jakobsen, U. Olsbye, N. Guillou, C. Lamberti, S. Bordiga and K. P. Lillerud, *J. Am. Chem. Soc.*, 2008, **133**, 13850-13851.
171. D. Feng, Z. Y. Gu, J. R. Li, H. L. Jiang, Z. Wei and H. C. Zhou, *Angewandte Chemie*, 2012, **51**, 10307-10310.
172. J. E. Mondloch, W. Bury, D. Fairen-Jimenez, S. Kwon, E. J. DeMarco, M. H. Weston, A. A. Sarjeant, S. T. Nguyen, P. C. Stair, R. Q. Snurr, O. K. Farha and J. T. Hupp, *Journal of the American Chemical Society*, 2013, **135**, 10294-10297.
173. H. Furukawa, F. Gándara, Y.-B. Zhang, J. Jiang, W. L. Queen, M. R. Hudson and O. M. Yaghi, *Journal of the American Chemical Society*, 2014, **136**, 4369-4381.
174. V. Guillermin, M. F. Ragon, Dan-Hardi, T. Devic, M. Vishnuvarthan, B. Campo, A. Vimont, G. Clet, Q. Yang, G. Maurin, G. Férey, A. Vittadini, S. Gross and C. Serre, *Angew. Chem. Int. Ed.*, 2012, **51**, 9267-9271.
175. X. Liang, F. Zhang, W. Feng, X. Zou, C. Zhao, H. Na, C. Liu, F. Sun and G. Zhu, *Chemical Science*, 2013, **4**, 983.